AUSTRIAN
MARSHALL PLAN FOUNDATION
VIENNA | AUSTRIA

TNFR1 - a Mechanistic Link between Cardiac Inflammation and Fibrosis

Magdalena Mayr

Baylor College of Medicine, Houston, TX

August 2014- August 2015

Supervised by:

Dr. Sandra Haudek

Dr. Martina Marchetti-Deschmann

TECHNISCHE UNIVERSITÄT WIEN
Vienna University of Technology

Baylor College of Medicine

ABSTRACT

Background: Brief systemic infusion of Angiotensin-II (Ang-II) to wild-type (WT) mice initiates the development of cardiac interstitial fibrosis. Genetic deletion of tumor necrosis factor alpha receptor-1 (TNFR1) obviates this development and concurrently inhibits Ang-II-induced cardiac hypertrophy and remodeling. Ang-II is also a major regulator of kidney function, but the contribution of TNFR1 signaling to renal health is unknown. Therefore, we now investigated the long-term effects of Ang-II and TNFR1 signaling on the heart, kidney, and cardiorenal function.

Methods: WT and TNFR1-knockout (TNFR1-KO) mice were infused with 1.5 μg/kg/min Ang-II for 1 and 6 weeks. Heart, kidney, and serum were isolated and evaluated by histologic, immunohistochemical, cytometric, quantitative PCR, and enzymatic measurement methods. Cardiac remodeling and function was determined by 2D-directed M-mode echocardiography and Doppler ultrasound, systolic blood pressure by tail-cuff plethysmography.

Results: Brief infusion of Ang-II to WT mice did not evoke a fibrotic response in the kidney. However, after 6 weeks, WT kidneys developed minimal, but significant interstitial collagen deposition which was supported by upregulation of collagen type I and III, and α-smooth muscle actin gene activation. This fibrotic development was associated with the appearance of myeloid fibroblast precursors, pro-inflammatory M1 and pro-fibrotic M2 cells, and myofibroblasts. Transcriptional expression of pro-inflammatory and pro-fibrotic genes was also increased. These changes were not seen in Ang-II-infused TNFR1-KO kidneys. In WT hearts, despite the disappearance of myeloid cells, cardiac fibrosis persisted throughout the 6-week infusion. At this time point, WT hearts generally maintained systolic and diastolic function, however, they developed clear evidence of accelerated cardiac hypertrophy and remodeling. Again, these changes were less prominent in Ang-II-infused TNFR1-KO hearts. By contrast, both WT and TNFR1-KO mice responded identically with similar elevations of systolic blood pressure, serum blood urea nitrogen, and serum creatinine levels.

Conclusions: Ang-II-infusion induced an immediate fibrotic response in the heart while fibrosis in the kidney developed slowly; both were initiated by chemokine-driven uptake of myeloid fibroblast precursor cells. The cardiac fibrosis was accompanied by progressive adverse remodeling. TNFR1-KO mice were protected from the Ang-II-induced cardiac and renal fibrosis, despite similar increases in blood pressure and renal dysfunction.

INDEX

1. INTRODUCTION

1.1 Heart Disease

Heart disease is worldwide the leading cause of death and is responsible for 17.3 million deaths each year.[1] In Europe alone 46% of all deaths are caused by cardiovascular disease.[2] Chronic hypertension, injury to the myocardium, and congenital heart disease may all lead to cardiac dysfunction characterized by hypertrophy, changes in size, shape, and structure (remodeling), and changes in physiology.[3] Cardiac remodeling is initially an adaptive response to injury to maintain normal cardiac function, however, over time it can become maladaptive and cause progressive cardiac decompensation.[4] Cardiac fibroblasts play a key role in regulating adaptive and maladaptive myocardial remodeling.[5] On one hand, fibroblasts are important producers of collagen, an extra cellular matrix (ECM) protein that builds up connective tissue and thus keeps cells together, necessary to maintain normal cardiac function. On the other hand, too much collagen deposition (fibrosis) can increase tissue stiffness and thereby impair ventricular function. In the case of acute injury, such as myocardial infarction in which myocytes die due to lack of oxygen, collagen and other ECM proteins are deposited to replace dead tissue (scar formation). This type is generally regarded as adaptive or reparative fibrosis.[6] In other situations, for example during chronic diseases in which there is no obvious cell death, excessive matrix production in between live myocytes is called non-adaptive or reactive fibrosis.[7]

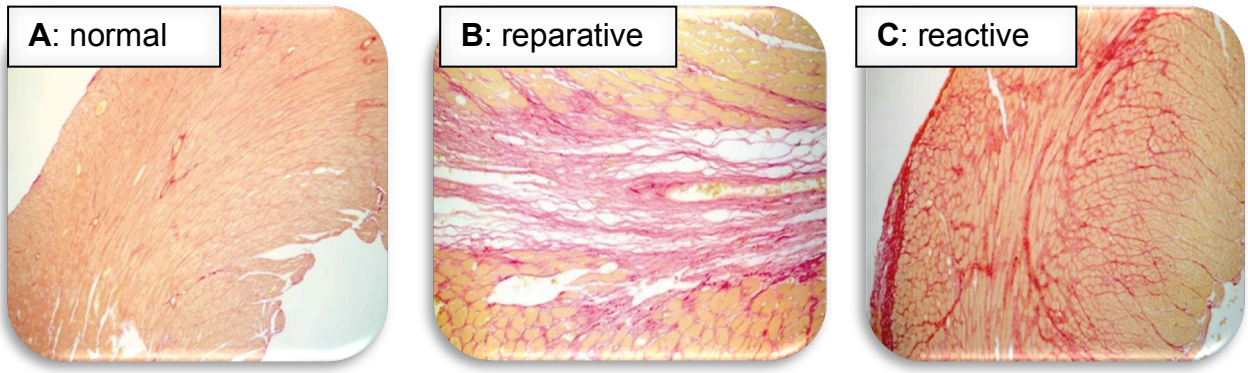

Figure 1: Different Types of Cardiac Fibrosis
Tissue sections were stained with picosirius red to determine collagen deposition (dark red). **A)** A healthy heart shows a normal amount of collagen deposition. **B)** Reparative fibrosis develops in response to acute injury: collagen is deposited to replace dead tissue. **C)** Reactive fibrosis: Collagen is deposited in between live cells in the absence of cell death.

Many chronic cardiac pathologies are associated with cardiac remodeling. Our previous studies using two different mouse models have shown that non-adaptive or reactive fibrosis is initiated by activated fibroblasts (myofibroblasts) of monocytic origin.[8,9,] Cardiac fibroblasts may be activated to secrete collagen by vasoactive proteins such as Angiotensin-II (Ang-II), as well as by pro-inflammatory cytokines such as tumor necrosis factor-alpha (TNF), interleukin-6 (IL-6), interleukin-1 (IL-1), and transforming growth factor beta (TGF-β). The levels of these parameters are increased in the remodeling heart.[5]

1.2 Angiotensin-II

The peptide hormone Angiotensin-II (Ang-II) plays an important role in the pathogenesis of cardiovascular diseases. Its synthesis is mainly regulated by the kidney as part of the Renin-Angiotensin-Aldosterone-System (RAAS) and controls the saltwater homeostasis, vascular tone, and blood pressure.[10] Initially, it was thought that Ang-II is primarily responsible for the constriction of vascular smooth muscle cells and the reabsorption of sodium. Yet, recent studies have shown that Ang-II also regulates important cellular immune responses, such as activation of pro-inflammatory transcription factor NF-κB (nuclear factor kappa-light-chain-enhancer of activated B cells).[11] NF-κB stimulates the expression of chemokines, such as monocyte chemoattractant protein-1 (MCP-1) that attracts monocytes and macrophages to the heart. NF-kB also mediates the release of pro-fibrotic mediators such as TGF-β from macrophages;[12] activation of TGF-β was shown to stimulate the production of extracellular matrix and thereby the development of fibrosis.[13] Therefore, Ang-II has been shown to be involved in both pro-inflammatory and pro-fibrotic processes.

1.3 Monocyte Chemoattractant Protein-1

Previous studies in our laboratory have shown that short-term infusion of Ang-II to wild-type (WT) mice resulted in interstitial cardiac fibrosis which was associated with induction of monocyte chemoattractant protein-1 (MCP-1), tumor necrosis factor-alpha (TNF) and the appearance of monocytic fibroblast precursors in the heart.[9,14]

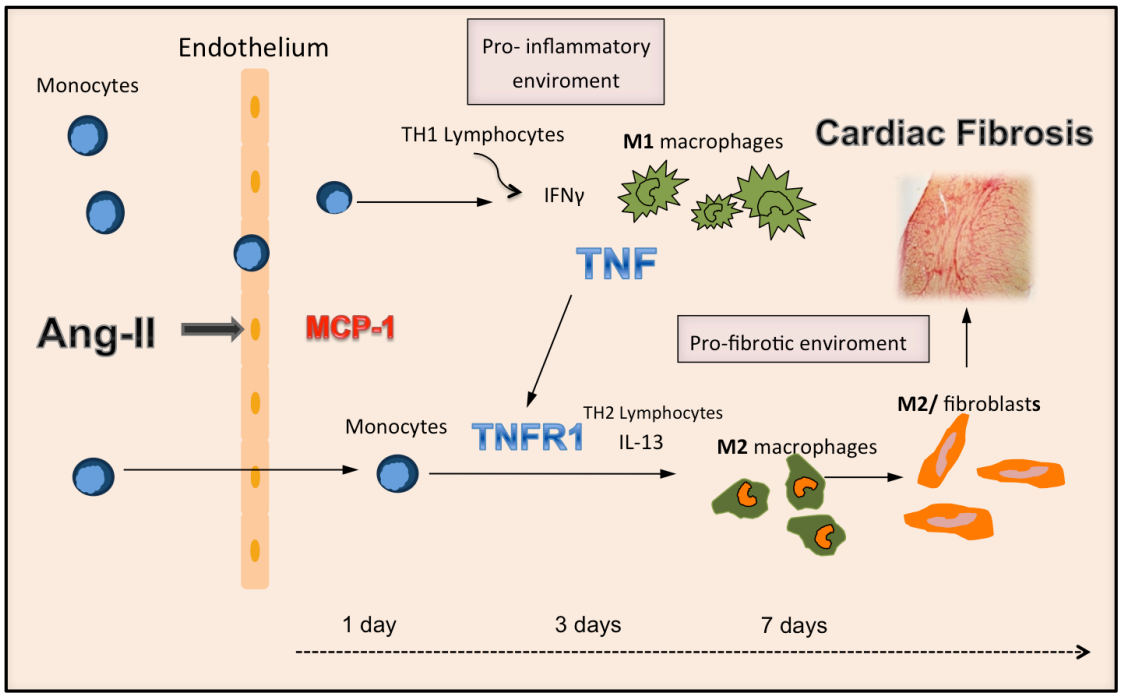

Figure 2: Monocytic Precursors Differentiate into Pro-inflammatory M1 and Pro-fibrotic M2 Cells[15]
Monocytic precursor cells migrate in response to MCP-1 to the heart where they mature into pro-inflammatory macrophages and pro-fibrotic M2 macrophages/fibroblasts depending on the surrounding environment.

Specifically, the non-adaptive fibrosis in response to Ang-II was initiated by migration of $CD34^+$ (marker of primitive cells) and $CD45^+$ (marker of hematopoietic cells) fibroblast precursor cells to the heart in response to MCP-1.[9] In the heart, some of the monocytes differentiated into M1 cells ($CD86^+CD45^+$) in a pro- inflammatory environment, whereas later migrating cells became $CD45^+$ M2 cells ($CD301^+$, $CD206^+$, $CD150^+$) as a pro-fibrotic response.[15] In mice lacking MCP-1 (MCP-1 knockout (KO) mice), the presence of this cell population and the development of fibrosis was obviated, despite cardiac remodeling.[9] Among many factors that were measured, TNF levels were upregulated in the WT heart by Ang-II infusion, suggesting that TNF was produced by infiltrating cells. The TNF synthesis was absent in MCP-1-KO mice.

1.4 Tumor Necrosis Factor-alpha

Tumor necrosis factor-alpha (TNF) is a pro-inflammatory cytokine and a major regulator of inflammation and immunity. It has beneficial effects in infectious diseases and is important for organogenesis.[16] However, the long-term expression or acutely high levels of TNF are deleterious.[17,18] TNF can bind to two receptors, 55-kDa TNF receptor type 1 (TNFR1) and 75-kDa TNF receptor type 2 (TNFR2)[16]. TNFR1 is better characterized than TNFR1. TNFR2 is mainly found on cells of the immune system, whereas TNFR1 is present on almost every tissue and has an important role in cell differentiation, activation, and apoptosis. TNFR1 is thought to mediate mostly

deleterious mechanisms, while TNFR2 is thought to be important for protective effects.[19,20]

Clinical trials of global TNF blockade to treat adverse cardiovascular events have unexpectedly failed and thus cast doubt on the precise role of its function. One major explanation was found in the divergent signaling response of the two TNF receptors TNFR1 and TNFR2.[20] Data for TNF in fibrotic diseases are in part contradictory and do not allow definite conclusions about its role in fibrosis.[21]

1.5 Previous Studies

To study the mechanism between Ang-II, MCP-1, and TNF we chose to use mice deficient in TNF signaling (either TNFR1 or TNFR2 deficient mice) and exposed them to Ang-II. Our data suggested that Ang-II-induced TNF initiated cardiac fibrosis by signaling through TNFR1; the genetic deletion of TNFR1, but not of TNFR2, obviated the development of fibrosis after short-term Ang-II infusion.[14,15]

To confirm the hematopoietic origin of fibroblast precursor cells we performed bone marrow transplantation experiments.[8,15] In our most recent study, TNFR1-KO mice were irradiated and their bone marrow was reconstituted with WT cells to produce chimeric TNFR1-KO/WT mice. Upon Ang-II exposure, chimeric TNFR1-KO/WT mice developed the same severity of cardiac fibrosis than WT mice, mediated by cardiac uptake of $TNFR1^{+}$ (WT) cells that were positive for fibroblast markers, indicating their commitment to a fibroblast lineage.[15] These observations suggested that the fibroblast precursor cells in our model were of bone marrow origin and supported our previous results that the signaling for the uptake and/or maturation into myofibroblasts occured through TNFR1 signaling. [14,15]

2. HYPOTHESIS

In our current study, we investigated 2 hypotheses:

1) We hypothesized that even after long-term infusion of Ang-II, mice deficient in TNFR1 signaling are protected against reactive cardiac fibrosis and remodeling.

2) We hypothesized that the development of Ang-II-induced renal fibrosis is also regulated by TNFR1 signaling.

To investigate our hypotheses, we utilized TNFR1-knockout mice (TNFR1-KO) for short- and long-term Ang-II infusion and characterized effects on heart, kidney, and cardiorenal function.

To support our in vivo data we further performed in vitro transendothelial migration assays to specifically characterize the monocyte-to-fibroblast differentiation. We have developed this assess previously using human monocytes,[22,23] and lately monocytes isolated form mouse spleen.[15]

3. METHODOLOGY

3.1 Animals

C57BL/6-Tnfrsf1a^{tm1Imx}/J (TNFR1-KO) and C57BL/6J (WT) mice (both from The Jackson Laboratory) were infused with 1.5 µg/kg per minute Ang-II via subcutaneously implanted osmotic pumps (ALZET®) for 1 and 6 weeks.[24] Control animals received saline. The euthanization was performed by cervical dislocation under 2% isoflourane. All experiments were conformed to the *Guide for the Care and Use of Laboratory Animals* published by the National Institutes of Health. The treatment of the mice was according the guidelines of the Baylor College of Medicine Animal Care and Research Advisory Committee.

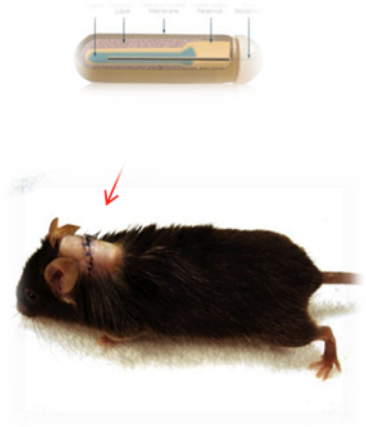

Figure 3: Mouse with Subcutaneously Implanted Osmotic Pump

3.2 Tissue Staining

Hearts were perfusion-fixed in Zinc-Tris buffer, paraffin embedded and cut in 5 µm thick sections at the mid-papillary level.[8,9,14] Kidneys were either perfusion-fixed or frozen in Tissue Tek ® Optimal Cutting Temperature (O.C.T.) at -80°C and placed on Tissue Tek® Cryomolds®. Kidneys were cut from the middle plane. All tissue sections were mounted in Cytoseal XYL after the staining process. Four images per stained section, with 4-6 sections per mouse, were captured with a 10x magnification on an Olympus.CKX41 inverted microscope using QcapturePro 5.0 for qualitative analysis.

3.2.1 Trichrome Staining

Trichrome staining was used for histological visualization of collagenous connective tissue fiber. Frozen sections were allowed to thaw for 30 minutes before they were stained according to the protocol of the Trichrome Stain Kit (Modified Masson's) from Diagnostic BioSystems (KT 034-IFU). Images of the stained slides were evaluated by two independent, blinded investigators using a score; 0= no collagen deposition, 1= minor, 2= medium I, 3= medium II, 4= severe collagen deposition.

3.2.2 Picrosirius Red Staining

Picrosirius red staining was used to determine the collagen deposition. Deparaffinized heart and kidney sections were stained with 0.05% picrosirius red for 1 hour and washed in two changes of acidified water. Afterwards, the tissue was dehydrated in three changes of 100% ethanol and cleared in xylene. The area of the collagen deposition was calculated as percentage of the total myocardial area or the total kidney area using the software Image-Pro Plus 5.1.

3.2.3 Periodic-acid Schiff Staining

Periodic-acid Schiff staining was performed to investigate the structure of the glomeruli and the renal tubular to see changes in cellularity, membrane thickness or signs of scaring in the interstitium. The kidney slides were stained according to kit instructions (Sigma-Aldrich, 395B-1KT) and evaluated by two independent, blinded investigators.

3.2.4 Mac-2, CD68, and α-SMA Immunostaining

Perfusion-fixed sections were deparaffinized, dehydrated, and permeabilized with 1% Tween 20. The staining was performed with Vector Labs M.O.M Kit and 1µg antibody (Mac-2: Cedarlane), CD68: eBioscience), α-smoth muscle actin (α-SMA): Sigma-Aldrich). For detection we used the Vector Labs ABC detection kit and the DAB substrate kit (Vector Labs DAB peroxidase substrate kit). The Mac-2, CD68, and α-SMA positive stained cells were counted by two independent, blinded investigators using the software ImageJ. Mac-2 staining was performed to detect macrophages in heart tissue, CD68 to detect macrophages in the kidney.

3.3 RNA Isolation and mRNA Expression (Quantitative PCR)

Frozen tissues (whole heart, whole kidney) were grinded to powder with an RNAseZap treated mortar with some liquid nitrogen. The samples were transferred into 50 ml Falcon tubes with 2 ml Trizol Reagent (Life Technologies), which inhibits any low level RNAse activity. Additionally the tubes were placed on ice to prevent any nuclease activity. The following homogenization was carried out with a Polytron homogenizer until all tissue clumps were dissolved. After transferring the samples into 0.5 ml Eppendorf tubes the Trizol/tissue mixture was allowed to sit for 5 minutes at room temperature to dissolve proteins. Subsequently 200 µl chloroform was added to each tube and after mixing well, the samples were allowed to sit for 2-3 minutes at room temperature. After centrifugation at 12,000 g for 15 minutes at 4°C, the clear upper aqueous phase was transferred into two new 0.5 ml Eppendorf tubes and 1 ml isopropyl alcohol was added. The samples were inverted gently, and then remained undisturbed for 10 minutes at room temperature. The centrifugation step at 12,000 g for 10 minutes at 4°C pelleted the RNA, which was resuspended in 1 ml 75% ethanol, followed by another centrifugation step at 7,500 g for 5 minutes at 4°C. The ethanol was discarded and the pellet was set to air dry for 5–7 minutes. 100 µl of ultra-pure water was added and the samples were incubated for 10 minutes at 60°C to resuspend the RNA.

RNA concentration and purity were measured on a NanoDrop (Thermo Fisher Scientific). The $A_{260/280}$ should be about 2 and the $A_{260/230}$ not lower than 1.5. If necessary, the RNA sample was purified with the RNeasy Mini Kit (Qiagen) to increase the RNA yield and/or quality.

cDNA synthesis was performed according to the protocol of the Verso cDNA Kit (Thermo Scientific). The Real Time PCR was performed with IQ SYBR Green Super mix on an iQ5 cycler (Bio-Rad). The Gene expression was normalized to 18s ribosomal RNA levels. All primers were validated according to MIQE guidelines prior to their use.[25] Relative gene expression compared to control was calculated using the ΔΔCq method.

Primer	Sense	Antisense
18s RNA	5'-ACCCGCAGCTAGGAATAATGGA-3'	5′-GCCTCAGTTCCGAAAACCA-3′
TNF	5′-CCAGTGTGGGAAGCTGTCTT-3′	5′-AAGCAAAAGAGGAGGCAACA-3′
MCP-1	5′-TCCACAACCACCTCAAGCACTTC-3'	5′-GGCATCACAGTCCGAGTCACAC-3′
Collagen type I	5′-TGTTGGCCCATCTGGTAAAGA-3′	5′-CAGGGAATCCGATGTTGCC-3′
Collagen type III	5′-TGGTCCTCAGGGTGTAAAGG-3′	5′-GTCCAGCATCACCTTTTGGT-3′
CCR2	5′-GGGTCATGATCCCTATGTGG-3′	5′-TCCATGAGCAGTGGTTTGAA-3′
TGF-β1	5′-CACTGGAGTTGTACGGCAGT-3′	5′-AGAGCAGTGAGCGCTGAATC-3′
Periostin	5'-TGGTATCAAGGTGCTATCTGCG-3′	5'AATGCCCAGCGTGCCATAA-3′
TNFR1	5'-GCTGACCCTCTGCTCTACGAA-3′	5'-GCCATCCACCACAGCATACA-3′
TNFR2	5'-TGCGCCTTGAAAACCCATTC-3′	5'AATGCCCAGCGTGCCATAA-3′
IL-6	5'-TGCGCCTTGAAAACCCATTC-3′	5'-GAAGTAGGGAAGGCCGTGG-3′
IL-4	5'-CCTCACAGCAACGAAGAACA-3′	5'-ATCGAAAAGCCCGAAAGAGT-3′
IL-13	5'-GTGTCTCTCCCTCTGACCCT-3′	5'-GGGGAGTCTGGTCTTGTGTG-3′
IFN-γ	5'-ACTGGCAAAAGGATGGTGAC-3′	5'-GACCTGTGGGTTGTTGACCT-3′
Osteopontin	5'-TGATGACGATGATGATGAC-3′	5'-CTCAGTCCATAAGCCAAG-3′
α-SMA	5'-GCTGGACTCTGGAGATGG-3'	5'-GCAGTAGTCACGAAGGAATAG-3'
Endothelin-1	5'-GCACCGGAGCTGAGAATGG-3'	5'-GTGGCAGAAGTAGACACACTC-3'

Table 1: Primer Sequences

3.4. Blood Urea Nitrogen and Creatinine Measurements

Blood Urea Nitrogen (BUN) and Creatinine are metabolic end-products.[26] Urea is a product of the oxidation of amino acids and ammonia. Creatinine is hydrolyzed from creatin. Both are indicators for renal problems if they are present in the bloodstream in higher levels.[27]

BUN and Creatinine were measured in serum using enzymatic reaction kits (Sigma-Aldrich; MAK006, MAK080). Measurements were performed on a VersaMax plate reader (Molecular Devices). Blood was collected from mice after cervical dislocation. The blood was allowed to clot at room temperature for 30 minutes, then was centrifuged at 1,500 g for 10 minutes. The supernatant was centrifuged again at 12,000 g for 10 minutes. The serum samples were aliquoted and stored at -80°C.

3.5 Flow Cytometry

Flow Cytometry allows to measure cell size, granularity, and 2-4 different protein expression profiles using fluorescent-labeled antibodies/components to characterize physical and functional characteristics of isolated cells. To isolate cells, heart and kidney tissue were diced and enzymatically digested by 0.1 mg/ml LiberaseTH Research Grade (Roche). To stain extracellular proteins, $1x10^5$ cells were incubated with 50nm calcein (Molecular Probes). Calcein was used to distinguish between live and dead cells, because only living cells are able to metabolize calcein, thereby releasing a florescent product.

To stain intracellular proteins, saponin buffer was used for cell permeabilization and paraformaldehyde as fixative (Becton Dickinson).

The cells were then stained with 0.5 µg directly conjugated or biotin-conjugated external antibodies (Becton Dickinson) followed by phycoerythrin (PE)- or streptavidin-PE/cyanine-5 (PE/Cy5)- conjugated secondary antibodies (Becton Dickinson). Anti-collagen type I (Rockland) was conjugated with fluorescein isothiocyanate (FITC)-anti-rabbit antibody.

The FITC/PE/Cy5 fluorescence intensities were measured on a Beckman Coulter Epics XLMCL flow cytometer using EXPO32 software.

3.6 In vitro Monocyte-Fibroblast Differentiation Model (TransEndothelial Migration Assay, TEM)

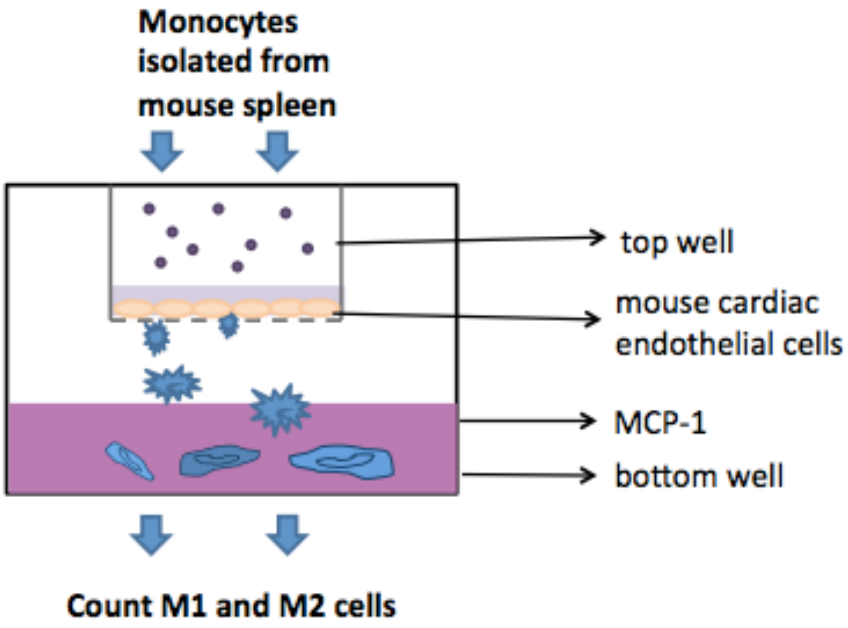

Figure 4: In vitro Monocyte-to-Fibroblast Differentiation Model
Isolated monocytes are placed into the top well and are allowed to migrate through a cardiac endothelial cell layer in response to MCP-1 into the bottom well where they adhere and mature. After 4 days of culture, the number of fibroblasts is counted.

3.6.1 Immortalized Mouse Cardiac Endothelial Cells (MCEC)

Immortalized Mouse Cardiac Endothelial Cells (MCEC) are microvascular neonatal mouse cardiac endothelial cells modified by transfection with lentiviral vectors carrying SV40 T antigen and human telomerase. This cell line is very suitable to investigate the mechanisms of wound healing and inflammation.[28]

The cells were cultured at 37ºC and 5.8-6.5 % CO_2 in Dulbecco's Modified Eagle's Media (DMEM; Gibco). 5% fetal bovine serum (FBS) was added to the medium which is an ideal cell grow supplement and HEPES (N-2-Hydroxyethylpiperazine-N-2-Ethane Sulfonic Acid), a buffering agent to maintain the pH in the medium. 10 mM penicillin and streptomycin prevented contaminations with bacteria and/or fungi.

The MCEC were grown in an adherent culture system in tissue culture-treated flasks to allow cell adhesion (Fisher Scientific). The cells had to be passaged every 4 days into a new flask. To do so, the old media was removed and the cells were washed with phosphate buffered saline (PBS) without calcium and magnesium (Gibco), because it would inhibit the effects of the ensuing dissociation reagent. The dissociation occurs enzymatically with 3 ml TrypLE Express (Life Technologies). After 3-4 minutes at 37ºC, when cells were detached, 7 ml of medium was added to inactivate the TrypLE. No other inhibitors were needed to stop the enzyme reaction, the dilution with the medium/serum was sufficient. The suspension was centrifuged at 1,200 rpm for 5 minutes at 4ºC to spin down the cells and resuspended in 50 ml medium with 5% FBS, before the cells were transferred to a new flask.

3.6.2 Isolation of Spleen Cells

Spleens from WT, TNFR1-KO, and C57BL/6-Tnfrsf2a^{tm1Imx}/J (TNFR2-KO; from The Jackson Laboratory) mice were used as monocyte source. Mice were euthanized with 2% isoflourane followed by cervical dislocation. The spleen was harvested and placed in ice-cold PBS in a petri dish on ice. It was very important to work with the organ immediately! 600 µl of a liberase digestion buffer (500 µg/ml) with DNase (20,000 U/ml) (EMD) was added to the petri dish and the spleen was carefully diced with a scalpel. The tissue was then placed in a 1,5 ml Eppendorf tube. The petri dish was washed with another 400 µl of liberase digest buffer and transferred to the same tube. The tissue-buffer mix was incubated at 37ºC for 15 minutes in the incubator on a shaker to digest the spleen. Afterwards, the tissue was passed through an 18-gauge needle and again incubated at 37ºC for 15 minutes. A 70 micron cell strainer was placed on a 50 ml tube with 3 ml of DMEM Medium + 1% FBS and the tissue-liberase mix was passed through it. The strainer was washed with DMEM medium + 1% FBS and the volume was brought to a total of 10 ml. The cells were centrifuged at

300 g for 5 minutes at 4ºC, resuspended in 2 ml of 1x RBC Lysis Buffer (eBioscience) and incubated for 2 minutes at room temperature. A dilution with PBS to 15 ml was followed and the cells were pelleted again at 300 g for 8 minutes at 4ºC. After resuspending in 15 ml PBS another two washing/centrifugation steps were performed at 200 g for 10 minutes. The final spin occurred at 250 g for 10 minutes and the cells were resuspended in 10 ml of PBS + 1% FBS, before they were counted.

3.6.3 Isolation of Monocytes

To separate monocytes from other cells in the suspension, the EasySep mouse monocyte enrichment kit (Stem Cell Tech, 19761) was used. The principle of the kit is based on negative selection. The unwanted cells were labeled with biotinylated monoclonal antibodies against cell surface antigens (B cells, T cells, NK cells, dendritic cells, progenitors, granulocytes and red blood cells). Additionally two mouse IgG1 antibodies directed against biotin and dextran were used. Both antibodies are connected in bispecific Tetrameric Antibody Complexes (TAC) by rat monoclonal antibodies directed against mouse IgG1. The monocytes could then be separated from the unwanted cells by using magnetic dextran iron particles, which bind to the TAC-labeled cells.[29]

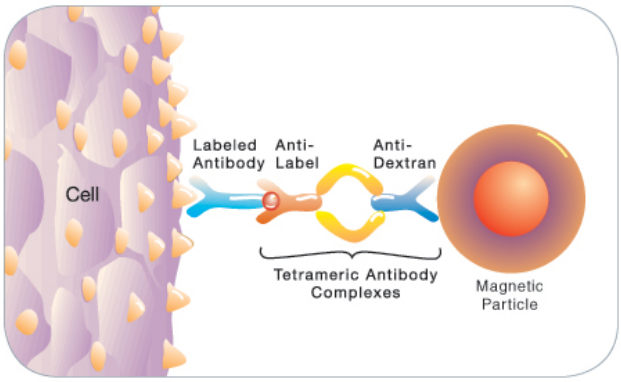

Figure 5: Schematic Drawing of Cell Labeling using EasySep Mouse Monocyte Enrichment Kit

A cell concentration of 1 x 10^8 cells/ml was prepared in PBS + 1% FBS and 1% rat serum (Stem Cell Tech). The rat serum was used to avoid non-specific binding of rat antibodies to mouse cells.[29] After isolating the monocytes from the cell suspension with the EasySep mouse monocyte enrichment kit, monocytes were resuspended in 1 ml of DMEM Medium supplemented with 1% FBS. The monocyte concentration was determined by using a hemocytometer.

3.6.4 Setup of the Transendothelial Migration Assay

300 µl (350,000- 400,000) endothelial cells were transferred into the top inserts of a 24-well plate. For the in vitro assay, cells were cultured in media with 1% FBS. A higher percentage of FBS was not necessary, because the goal was not to increase the cell number, but to close the endothelial cell layer in the top well. The cells were allowed to incubate for 6 days at 37ºC. After 6 days, the old media was suctioned off very carefully without destroying the endothelial layer in the top well. Then, 100 µl with 25 x 10^4 monocytes were added to atop of the endothelial call layer. Additionally 1 ng/ml of Ang-II (Sigma- Aldrich) and 10 ng/ml of TNF (R&D Systems) were pipetted into the top well. RPMI 1640 media was added to a total volume of 300 µl. In the bottom well 650 ng/ml of mouse MCP-1 (R&D Systems) was added to media. Control setups did not received Ang-II and TNF in the top well. After 4-6 days the top well was removed and 200 µl of 4% paraformaldehyde was added to fix the cells. After 20 minutes of incubation, cells were rinsed with tap water, and then stained with 500 µl Giemsa stain for 10 minutes. The wells were washed with distilled water and allowed to air dry for a day before counting. Each setup was measured in triplicates. Absolute amounts of spindle-shaped, purple stained fibroblasts per well were counted by two investigators using an Olympus.CKX41 microscope.

3.7 Noninvasive Functional Assessments

Baseline noninvasive Doppler ultrasound and 2-D-directed M-mode echo-cardiographic studies were performed before Ang-II exposure (baseline) and repeated after 6 weeks of Ang-II infusion to evaluate changes in cardiac function and remodeling.

All studies were performed on anesthetized mice under 1% isoflourane in oxygen at a rate of 2 L/min. Mice were first placed in anesthesia chambers until recumbent to be later placed on a 39°C heated ECG board to maintain normal body temperature. The mouse was placed in a supine position with its limbs taped to copper electrodes to monitor and maintain the heart rate between 400-500 beats per minute; anesthesia was continuously given via a nose cone. Body fur was shaved from the anterior thorax and abdominal area and acoustic gel was applied to perform the noninvasive measurements.

Functional and structural echocardiographic parameters of the left ventricle were obtained using a RMV 710B scan head and analyzed using Vevo 770™ VisualSonics software (Visualsonics). 2-D and M-mode images at the level of the left ventricle's papillary muscles were obtained to assess left ventricular wall thickness, end diastolic and end-systolic volumes, as well as fractional shortening and ejection fraction. The

images were all obtained at the level of the midpapillary muscles of the left ventricle to ensure standardization.

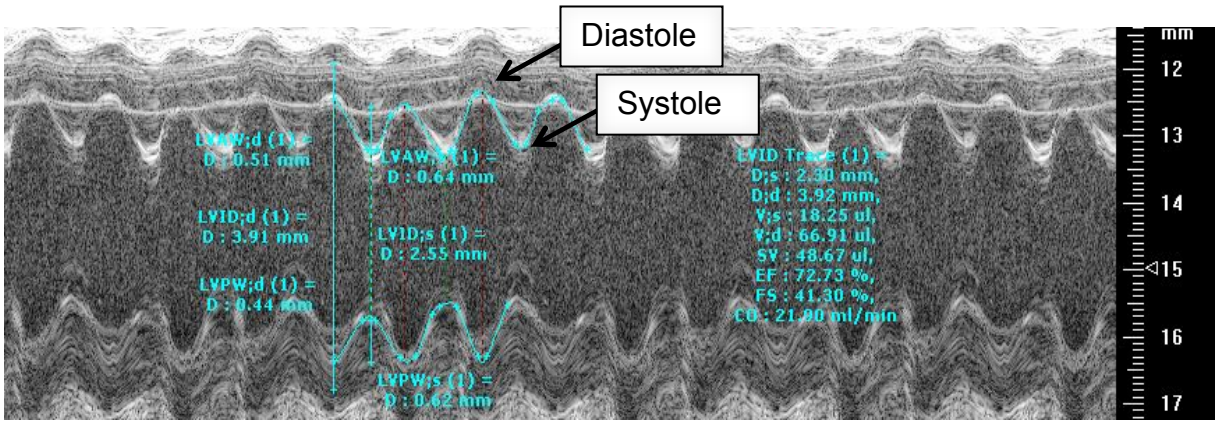

Figure 6: Representative M-Mode Echocardiography Image
The M-Mode image shows motion sequences three-dimensional and allows the evaluation of structural changes of the heart.

Additional functional cardiac parameters such as E-Peak Velocity, Isovolumic Contraction Time, and Isovolumic Relaxation Time were assessed by obtaining Doppler ultrasound signals from the aortic root and the mitral inflow tract using a 10-MHz probe and analyzed using a real-time signal acquisition and spectrum analyzer system, Doppler Signal Processing Workstation (DSPW, Indus Instruments).

Systolic Blood Pressure was measured before and after Ang-II infusion (at 1, 2, 4, 6, weeks) by tail-cuff plethysmography (Visitech Systems) which is a light- based technology method. Mice were placed in a preheated chamber (39°C) and the tail was put in a cuff with a LED light source. The light records the pulse signal wave by measuring the vessel dilation caused by pulsatile variations in blood volume and sends the light intensity to a detector.[30] An acclimatization phase of one week daily measurements was necessary to train mice before an accurate SBP baseline measurement was recorded.

Figure 7: Blood Pressure Analyzer
Blood pressure was measured by tail-cuff plethysmography (Visitech Systems) to investigate the effect of Ang-II on the blood pressure in WT and TNFR1-KO mice.

3.8 Statistics

Kolmogorov-Smirnov tests were used to evaluate normal distribution, Bartlett's tests to evaluate differences among Standard Deviations. Unpaired two-tailed Student's t-tests (or Mann-Whitney if nonparametric) were used to compare differences between 2 groups. One-way ANOVA (or Kruskal-Wallis if nonparametric) were used to compare differences between >2 groups; Tukey-Kramer post-hoc testing (or Dunn's if nonparametric) were performed when appropriate. A P-value <0.05 was considered statistically significant (GraphPad InStat 3.06). Data in text, tables, and figures express mean ± SEM.

4. RESULTS

4.1 Histological Changes after Ang-II Infusion

Kidney: WT and TNFR1-KO mice were infused with Ang-II. No histological changes were observed in the kidney after 1 week; however, after 6 weeks tubule-interstitial collagen deposition was significantly increased. Figure 8.A1 shows representative Trichrome staining of frozen kidney sections. WT mice show a larger blue area (stained collagen) after 6 weeks of Ang-II exposure compared to TNFR1-KO kidneys. For quantitative analysis we used a score from „0“- indicating no collagen to „4“- indicating severe collagen deposition; the results are shown in Figure 9.A2. Further, the number of α-smooth muscle actin^{+} cells (α-SMA; a marker for activated fibroblasts) increased after 6-week Ang-II infusion in the WT kidney (Figures 8.B1- qualitative, 9.B2- quantitative), whereas there was no change in the TNFR1-KO kidney. Similarly, the amount of CD68^{+} cells (marker of macrophages) increased in WT, but not in TNFR1-KO kidneys (Figures 8.C1- qualitative, 9.C2- quantitative) after 6 weeks of Ang-II infusion. Lastly, we performed PAS staining to characterize the overall changes of the kidney. We found no significant changes in mesangial proliferation, necrosis, and morphology after 6 weeks of Ang-II treatment (Figure 8.D1- qualitative).

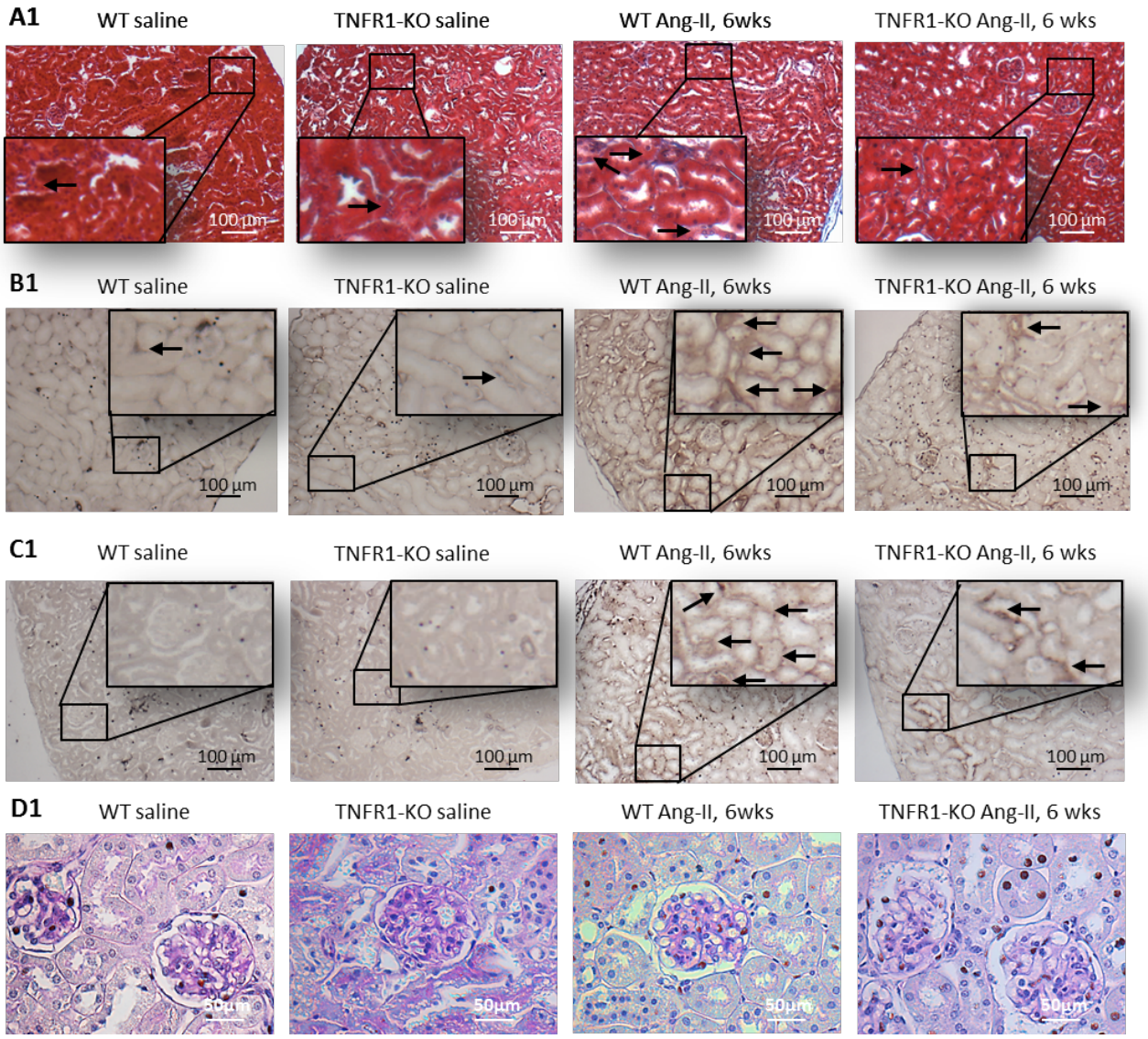

Figure 8: Representative Images of Stained Kidney Tissue
(A1) Trichrome staining shows collagen deposition as blue areas. WT kidneys developed fibrosis after 6 weeks of Ang-II infusion, whereas TNFR1-KO kidneys did not. Immunohistochemistry staining indicated that **(B1)** αSMA^{+} cells (activated fibroblasts) and **(C1)** $CD68^{+}$ cells (macrophages) were increased in WT, but not in TNFR1-KO kidney in response to Ang-II infusion. **(D1)** PAS staining indicated no difference in mesangial proliferation, necrosis, and morphology between WT and TNFR1-KO kidneys with or without Ang-II infusion.

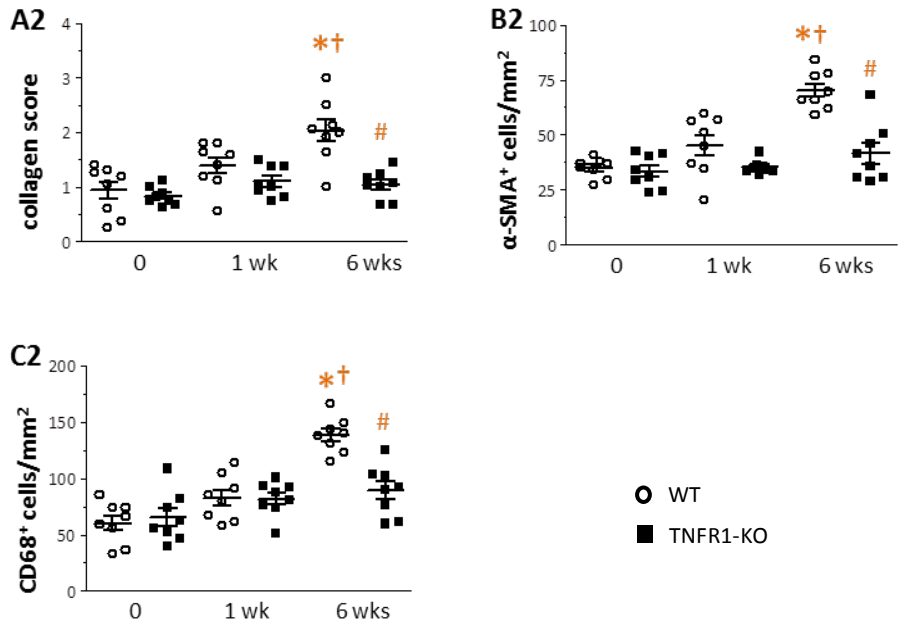

Figure 9: Quantitative Data from Stained Kidney Tissue
(A) Collagen deposition was increased in WT kidneys after 6 weeks of Ang-II infusion, but not in TNFR1-KO mice. **(B)** The number of α-SMA$^+$ cells, a marker for activated fibroblasts and **(C)** number of CD68$^+$ cells (macrophage marker) were increased after 6 weeks of Ang-II exposure in WT, but not in TNFR1-KO kidney. N=8/group. * P< 0.05 between saline and indicated time point within the same genotype group. † P< 0.05 between 1 week and 6 weeks within the same genotype group. # P< 0.05 between WT and TNFR1-KO at the same time point.

Heart: We have previously shown that collagen deposition after 1 week of Ang-II treatment was increased in WT, but not in TNFR1-KO hearts.[14,15] We now evaluated collagen deposition after 6 weeks of Ang-II infusion. We found that in WT hearts, the degree of fibrosis at 6 weeks was similar to the degree found at 1 week, indicating that collagen deposition neither diminished nor increased over time (Figure 10.A1- qualitative, Figure 11.A2- quantitative). Mice deficient in TNFR1 signaling remained protected from the Ang-II exposure and even after 6 weeks showed comparable collagen deposition to their corresponding saline-treated group. Similarly, the numbers of α-SMA$^+$ myofibroblasts (Figures 10.B1 and 11.B2) and Mac-2$^+$ macrophages (Figures 10.C1 and 11.C2) increased significantly after 6 weeks of Ang-II infusion in the WT mice, but not in the TNFR1-KO mice.

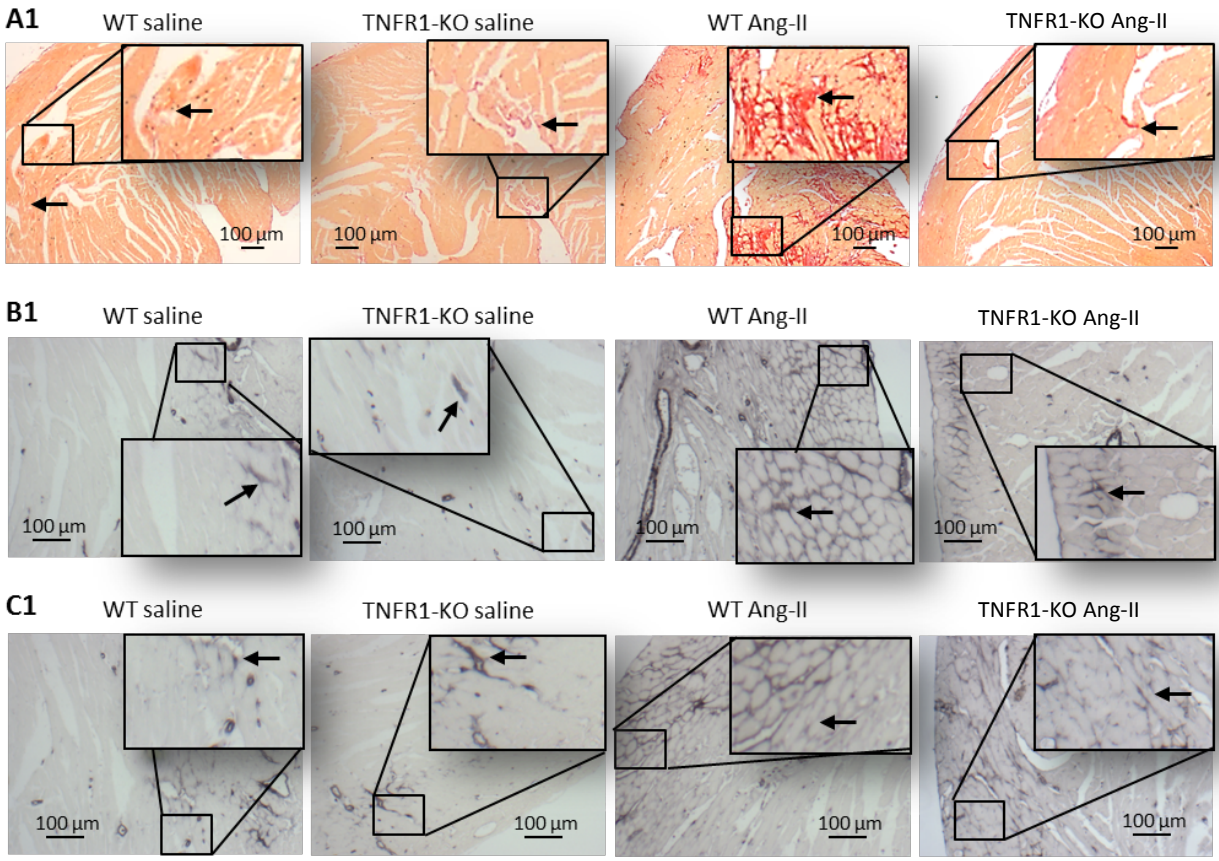

Figure 10: Representative Images of Stained Heart Tissue
(A1) Picrosirius red staining of mouse heart after 6 weeks of Ang-II infusion. WT mice developed significant cardiac fibrosis, whereas mice deficient in TNFR1 signaling did not develop fibrosis and also expressed **(B1)** fewer α-SMA^{+} and **(C1)** Mac-2^{+} cells than WT hearts.

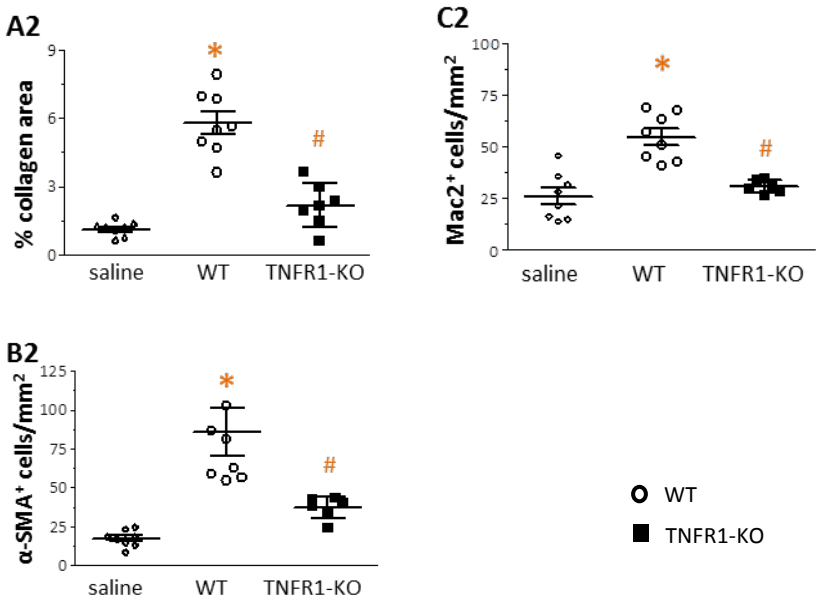

Figure 11: Quantitative Data from Stained Heart Tissue
(A) Increase of collagen deposition in WT hearts after 6 weeks of Ang-II infusion compared to no increase in TNFR1-KO hearts. **(B)** The number of α-SMA^{+} stained cells, a marker for activated fibroblasts increased after 6 weeks of Ang-II exposure in the WT mice, but not in the TNFR1-KO hearts. **(C)** CD68^{+} expressing cells were highly present in WT hearts, but not in TNFR1-KO hearts in response to Ang-II. Data for WT (n=4) and TNFR1-KO (n=4) saline groups were pooled for clarity, as there were no differences. WT and TNFR1-KO: N=6-8/group. *P< 0.05 between saline and Ang-II-treated groups. # P< 0.05 between WT and TNFR1-KO groups at 6 weeks of Ang-II treatment.

4.2 Expression of Pro-fibrotic and Pro-inflammatory Genes after Ang-II Infusion

Kidney: After 1 week of Ang-II infusion, the expression of fibrosis-related genes (collagen type I and III, TGF-β1, osteopontin, periostin, endothelin-1) was not significantly upregulated in the WT kidney, except for α-SMA which showed a slight increase in the WT mouse group (Table 2). After 6 weeks of Ang-II infusion, significant higher expression levels were observed in the WT kidney, but not in kidneys of mice deficient in TNFR1 signaling (Table 2). Pro- inflammatory factors (TNF, IL-1β, IL-6, MCP-1, CCR2) were upregulated at 6 weeks in the WT, however, their expression levels in Ang-II-treated TNFR1-KO kidneys was not different than in saline-treated TNFR1-KO kidneys. TNFR1 and TNFR2 expression showed no increase (Table 3). Th1- and Th2- related lymphokines were not upregulated after Ang-II infusion at any time point measured (Table 4), except for IL-13 which was significantly higher expressed in both WT and TNFR1-KO kidneys after 6 weeks. In summary, the infusion of Ang-II increased transcriptional activation of fibrosis- and inflammation related genes in the WT kidney, but not in the TNFR1-KO kidney. By contrast, expression of lymphokines was not different between WT and TNFR1-KO groups, similar to our previous observations in the heart.[15]

Fibrosis-related Proteins

	WT	WT	WT	TNFR1-KO	TNFR1-KO	TNFR1-KO
Gene	**saline**	**1 week**	**6 weeks**	**saline**	**1 week**	**6 weeks**
Collagen type I	0.9 ± 0.1	2.0 ± 0.6	2.3 ± 0.2 *	0.9 ± 0.1	1.3 ± 0.2	0.9 ± 0.1 #
Collagen type III	1.0 ± 0.1	1.1 ± 0.3	1.8 ± 0.2 *	1.0 ± 0.1	1.1 ± 0.2	0.7 ± 0.1 #
α-SMA	1.0 ± 0.1	2.1 ± 0.4 *	3.6 ± 0.2 * †	1.0 ± 0.1	1.2 ± 0.2	1.8 ± 0.2 #
TGF-β1	1.0 ± 0.1	1.2 ± 0.2	1.7 ± 0.1 * †	1.0 ± 0.1	0.9 ± 0.1	0.9 ± 0.1 #
Osteopontin	1.0 ± 0.1	1.4 ± 0.3	1.7 ± 0.2	1.1 ± 0.1	1.3 ± 0.2	1.7 ± 0.3
Periostin	0.9 ± 0.2	1.4 ± 0.1	1.8 ± 0.1 *	1.0 ± 0.2	1.1 ± 0.1	1.1 ± 0.2 #
Endothelin-1	1.0 ± 0.1	1.4 ± 0.3	2.7 ± 0.1	0.9 ± 0.1	0.8 ± 0.1	1.2 ± 0.2

Table 2: Transcriptional Activation of Fibrosis-related Proteins in the Kidney
Data represent fold-increase over WT saline (N=8/group)
* P< 0.05 between saline and indicated time point within the same genotype group
† P< 0.05 between 1 week and 6 weeks within the same genotype group
# P< 0.05 between WT and TNFR1-KO at the same time point

Inflammatory Cytokines, Chemokines, and their Receptors

	WT	WT	WT	TNFR1-KO	TNFR1-KO	TNFR1-KO
gene	**saline**	**1 week**	**6 weeks**	**saline**	**1 week**	**6 weeks**
TNF	1.1 ± 0.1	1.4 ± 0.2	12.4 ± 3.3 *†	0.8 ± 0.1	0.6 ± 0.1	4.1 ± 1.2 #
TNFR1	1.0 ± 0.1	1.0 ± 0.2	1.2 ± 0.1	n/a	n/a	n/a
TNFR2	1.1 ± 0.2	1.4 ± 0.3	1.4 ± 0.2	1.3 ± 0.2	1.2 ± 0.1	1.4 ± 0.4
MCP-1	1.0 ± 0.1	1.8 ± 0.5	2.6 ± 0.4 *	0.9 ± 0.2	1.0 ± 0.3	1.0 ± 0.3 #
CCR2	1.1 ± 0.1	1.9 ± 0.5	2.8 ± 0.6 *	0.9 ± 0.1	1.0 ± 0.2	1.3 ± 0.2 #
IL-1β	1.2 ± 0.1	1.9 ± 0.4	2.3 ± 0.2 *	1.0 ± 0.1	1.1 ± 0.2	1.0 ± 0.1 #
IL-6	1.2 ± 0.1	1.7 ± 0.4	2.8 ± 0.6 *	1.1 ± 0.1	0.9 ± 0.1	1.2 ± 0.1 #

Table 3: Transcriptional Activation of Inflammatory Proteins in the Kidney
Data represent fold-increase over WT saline (N=8/group)
* P< 0.05 between saline and indicated time point within the same genotype group
† P< 0.05 between 1 week and 6 weeks within the same genotype group
# P< 0.05 between WT and TNFR1-KO at the same time point

Th1- and Th2- related Lymphokines

	WT	WT	WT	TNFR1-KO	TNFR1-KO	TNFR1-KO
Gene	**saline**	**1 week**	**6 weeks**	**saline**	**1 week**	**6 weeks**
IFN-γ	0.9 ± 0.2	0.6 ± 0.0	0.8 ± 0.1	1.0 ± 0.2	0.7 ± 0.1	0.7 ± 0.1
IL-4	1.0 ± 0.1	1.0 ± 0.2	1.7 ± 0.2	1.2 ± 0.1	0.8 ± 0.4	1.2 ± 0.3
IL-13	0.9 ± 0.1	1.3 ± 0.1	2.9 ± 0.6 *	0.9 ± 0.1	0.8 ± 0.2	2.4 ± 0.5 #

Table 4: Transcriptional activation of Lymphokines in the Kidney
Data represent fold-increase over WT saline (N=8/group)
*P< 0.05 between saline and indicated time point within the same genotype group
† P< 0.05 between 1 week and 6 weeks within the same genotype group
# P< 0.05 between WT and TNFR1-KO at the same time point

Heart: We have previously determined gene expression after 3 and 7-day Ang-II infusion in the heart.[15] We now extended our observations with characterizing gene expression after 6 weeks of Ang-II infusion. Fibrosis-related gene expression (collagen type I and III, α-SMA, TGF-β1, osteopontin, periostin, endothelin-1) significantly increased in WT hearts after 1 week of Ang-II infusion,[14] and were still upregulated after 6 weeks, but much less than after brief infusion with Ang-II of 1 week (Table 5). In hearts lacking TNFR1 signaling we found no significant increase in fibrosis-related protein expression (Table 5). Pro-inflammatory IL-1β, IL-6, and IFN-γ, although still elevated after 6 weeks, were several fold lower than levels at 1 week (Tables 6 and 7). Notably, TNF and MCP-1 mRNA transcription was not upregulated after 6 weeks in the WT heart (Table 6).

Fibrosis-related Proteins

	WT	WT	TNFR1-KO	TNFR1-KO
Gene	**saline**	**6 weeks**	**saline**	**6 weeks**
Collagen type I	1.0 ± 0.1	2.7 ± 0.4 *	1.3 ± 0.1	1.7 ± 0.2 #
Collagen type III	1.0 ± 0.1	2.9 ± 0.5 *	1.4 ± 0.2	1.8 ± 0.1 #
α-SMA	1.1 ± 0.1	2.5 ± 0.5 *	1.2 ± 0.2	1.2 ± 0.1 #
TGF-β1	1.0 ± 0.1	1.9 ± 0.1 *	1.1 ± 0.1	1.0 ± 0.1 #
Osteopontin	1.1 ± 0.1	4.2 ± 0.7 *	1.2 ± 0.3	2.1 ± 0.5 #
Periostin	1.0 ± 0.1	6.5 ± 1.1 *	1.1 ± 0.1	2.6 ± 0.5 #
Endothelin-1	1.0 ± 0.1	2.2 ± 0.4 *	1.3 ± 0.1	1.6 ± 0.3

Table 5: Transcriptional Activation of Fibrosis-related Proteins in the Heart
Data represent fold-increase over WT saline (N=8/group)
* P< 0.05 between saline and indicated time point within the same genotype group
† P< 0.05 between 1 week and 6 weeks within the same genotype group
# P< 0.05 between WT and TNFR1-KO at the same time point

Inflammation-related Genes

	WT	WT	TNFR1-KO	TNFR1-KO
Gene	**saline**	**6 weeks**	**saline**	**6 weeks**
TNF	1.1 ± 0.1	1.6 ± 0.2	1.6 ± 0.1	1.7 ± 0.4
TNFR1	1.0 ± 0.1	1.2 ± 0.2	n/a	n/a
TNFR2	1.1 ± 0.1	1.2 ± 0.2	1.1 ± 0.2	1.1 ± 0.0
MCP-1	1.0 ± 0.1	1.5 ± 0.3	1.1 ± 0.1	1.1 ± 0.2
CCR2	1.1 ± 0.2	1.8 ± 0.4	1.3 ± 0.1	1.1 ± 0.6
IL-1β	1.0 ± 0.1	7.0 ± 2.7 *	1.1 ± 0.2	1.3 ± 0.1 #
IL-6	1.2 ± 0.3	6.0 ± 1.6 *	1.0 ± 0.1	2.5 ± 0.4 #

Table 6: Transcriptional Activation of Inflammatory Proteins in the Heart
Data represent fold-increase over WT saline (N=8/group)
* P< 0.05 between saline and indicated time point within the same genotype group
† P< 0.05 between 1 week and 6 weeks within the same genotype group
# P< 0.05 between WT and TNFR1-KO at the same time point

Th1- and Th2- related Lymphokines

	WT	WT	TNFR1-KO	TNFR1-KO
Gene	**saline**	**6 weeks**	**saline**	**6 weeks**
IFN-γ	1.0 ± 0.2	2.6 ± 0.3 *	1.1 ± 0.1	3.0 ± 0.4 *
IL-4	1.0 ± 0.2	1.5 ± 0.4	1.4 ± 0.5	1.4 ± 0.6
IL-13	1.2 ± 0.4	1.9 ± 1.0	1.0 ± 0.2	1.3 ± 0.6

Table 7: Transcriptional activation of Lymphokines in the Heart
Data represent fold-increase over WT saline (N=8/group)
*P< 0.05 between saline and indicated time point within the same genotype group
† P< 0.05 between 1 week and 6 weeks within the same genotype group
# P< 0.05 between WT and TNFR1-KO at the same time point

4.3 Fibroblast Precursor, M1, and M2 Cells after Ang-II Infusion

Kidney: Because we did not find collagen deposition after 1 week (Figure 8 and 9), we only investigated 6-week Ang-II-infused kidneys. After 6 weeks of Ang-II infusion, the numbers of $CD34^{+}CD45^{+}$ fibroblast precursor cells (Figure 12.A), of $CD86^{+}CD45^{+}$ and $CD16^{+}CD45^{+}$ pro-inflammatory M1 cells (Figures 12.B1 and B2), and of $CD301^{+}CD45^{+}$, $CD206^{+}CD45^{+}$, and $CD150^{+}CD45^{+}$ pro-fibrotic M2 cells (Figures 12.C1, C2, and C3) were significantly increased in the WT kidneys, whereas there was no change of their cell numbers in mice lacking TNFR1 signaling. Further, M2 cells present in the WT kidney also expressed collagen type I (Figures 12.D1, D2, and D3). These cells were absent in the TNFR1-KO group after 6 week Ang-II exposure.

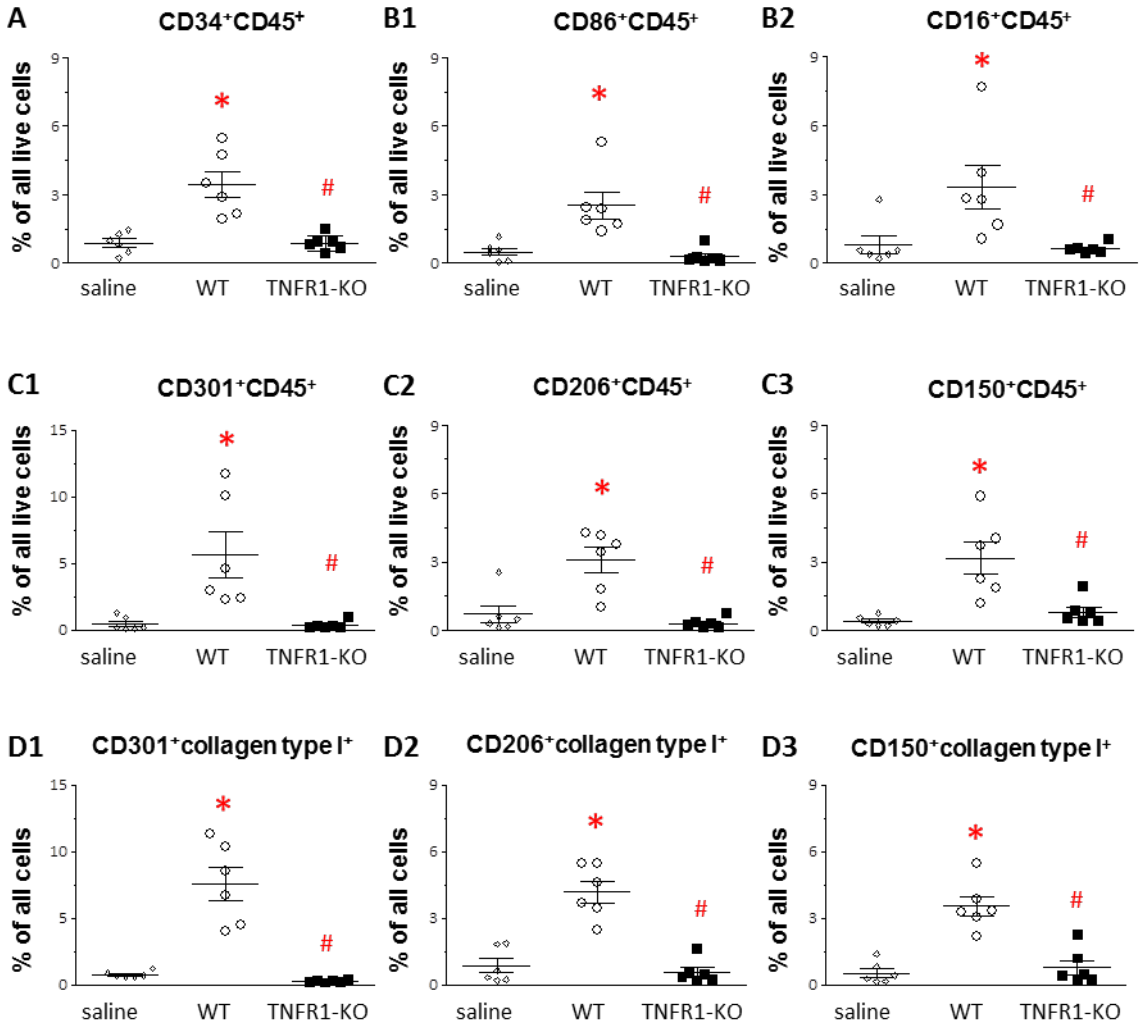

Figure 12: Flow Cytometric Analysis of Isolated Cells from the Kidney after 6 weeks of Ang-II Exposure
Live cells were identified via calcein uptake. **(A)** In the WT kidneys, monocytic fibroblast precursor cells ($CD34^+CD45^+$) were present after 6 weeks. **(B1, B2)** Pro-inflammatory M1 cells ($CD86^+CD45^+$ and $CD16^+CD45^+$), as well as **(C1, C2, C3)** pro- fibrotic M2 cells ($CD301^+CD45^+$, $CD206^+CD45^+$, and $CD150^+CD45^+$) were present in the WT, but not in the TNFR1-KO kidney. **(D1, D2, D3)** Collagen type I expressing M2 cells were also present in WT kidneys after 6 weeks; TNFR1-KO kidneys did not show an increase of these cell populations in response to Ang-II. Data for WT (N=3) and TNFR1-KO (N=3) saline groups were pooled for clarity, as there were no differences. WT and TNFR1-KO: N=6/GROUP. *P< 0.05 between saline and Ang-II-treated groups. # P< 0.05 between WT and TNFR1-KO groups at 6 weeks of Ang-II treatment.

Heart: We have previously shown a timely increase of fibroblast precursors, M1, and M2 cells after 3 and 7 days of Ang-II infusion.[15] We now found that after 6 weeks of Ang-II infusion, none of these cell populations were present in the heart. These findings indicate that the uptake of $CD34^+CD45^+$ fibroblast precursor cells (Figure 13.A), $CD86^+CD45^+$ and $CD16^+CD45^+$ pro-inflammatory M1 cells (Figures 13.B1 and B2), and $CD301^+CD45^+$, $CD206^+CD45^+$, and $CD150^+CD45^+$ pro-fibrotic M2 cells (Figures 13.C1, C2, and C3) in the WT initiate, but do not maintain fibrosis in the heart. Moreover these findings support our previous observations, that MCP-1 is necessary for their tissue uptake (see Table 6).

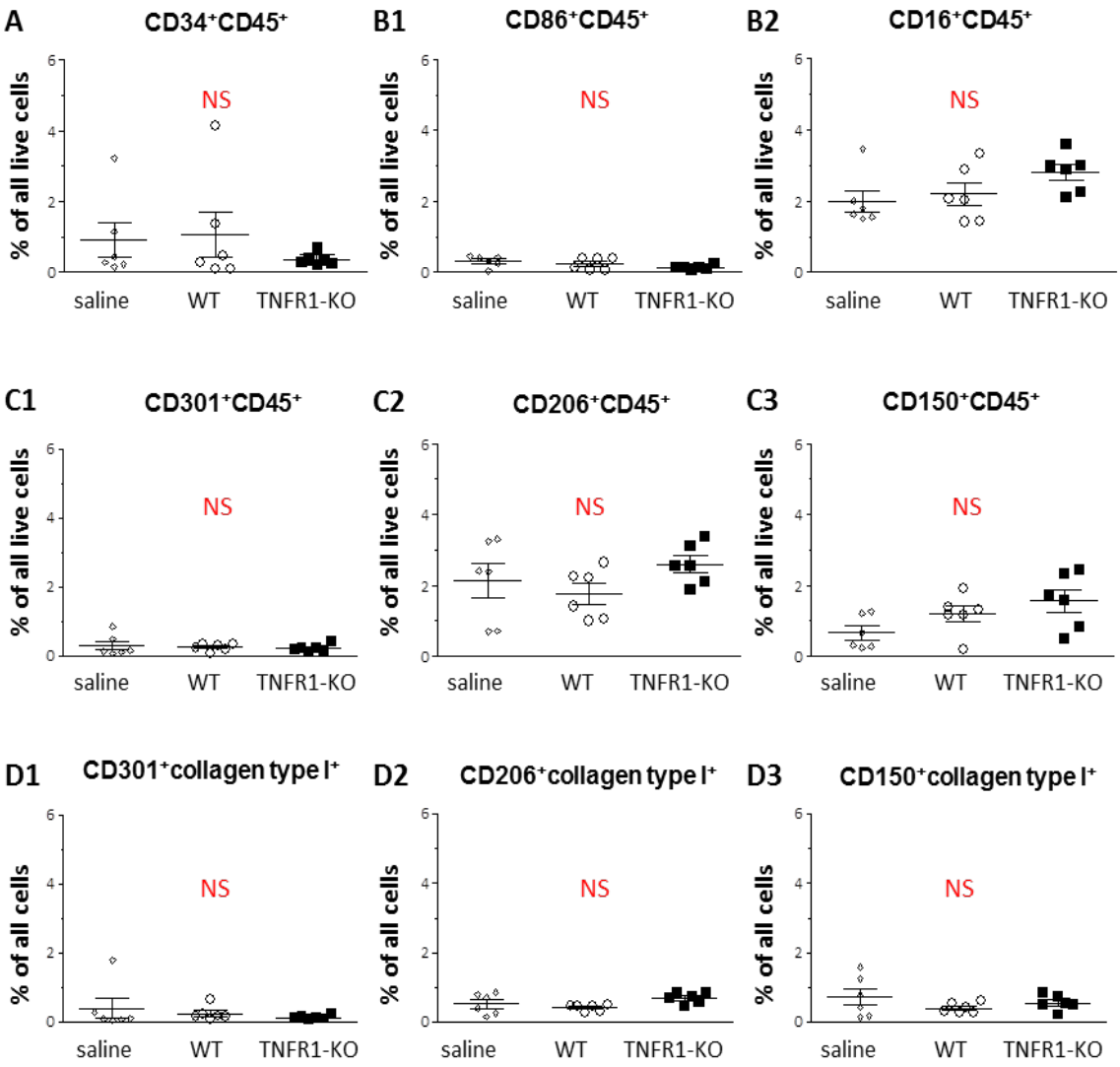

Figure 13: Flow Cytometric Analysis of Isolated Cells from the Heart after 6 weeks of Ang-II Exposure
Live cells were identified via calcein uptake. **(A)** Monocytic fibroblast precursor cells ($CD34^+CD45^+$), **(B1, B2)** pro-inflammatory M1 cells ($CD86^+CD45^+$, $CD16^+CD45^+$), and **(C1, C2, C3)** pro-fibrotic M2 cells ($CD301^+CD45^+$, $CD206^+CD45^+$, and $CD150^+CD45^+$) were not present in the WT, nor in TNFR1-KO hearts after 6 weeks of Ang-II infusion. **(D1, D2, D3)** Also Collagen type I expressing M2 cells were not present after 6 weeks. Data for WT (N=3) and TNFR1-KO (N=3) saline groups were pooled for clarity, as there were no differences. WT and TNFR1-KO: N=6/group. NS: no significance between saline, WT, and TNFR1-KO groups.

4.4 Effects of Ang-II Infusion on Kidney Function

Blood urea nitrogen (BUN) and creatinine levels measured in serum are useful indicators for renal function, as their serum levels rise as a result of renal failure.[27] In our experiments, both BUN (Figure 14.A) and Creatinine (Figure 11.B) levels increased in serum after 6 weeks of Ang-II infusion in the WT and TNFR1-KO mice to similar levels, indicating that both mouse groups developed kidney problems.

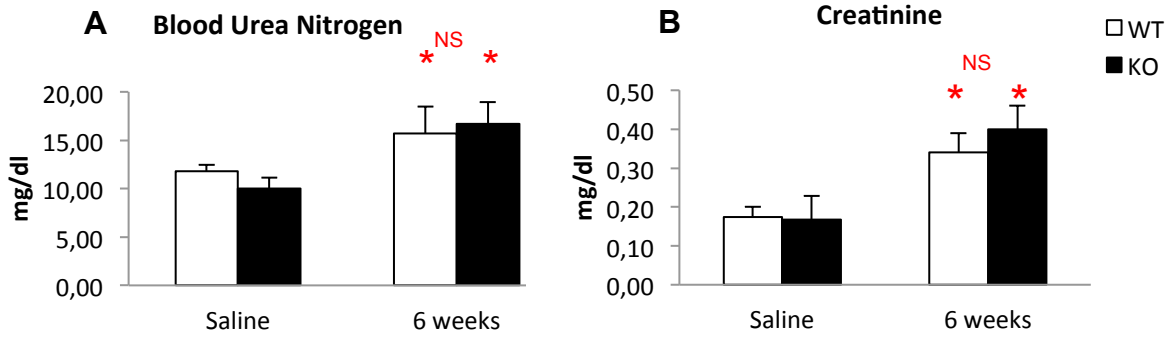

Figure 14: Renal Dysfunction
BUN and creatinine serum levels increased to similar extents in both WT and TNFR1-KO mouse groups, indicating the development of renal failure in both groups. N=8-10/group. *P< 0.05 between saline and 6-week time point within the same genotype group. NS: no significant difference between WT and TNFR1-KO at the same time point.

4.5 Effects of Ang- II Infusion on Blood Pressure and Cardiac Function and Remodeling

The WT mice responded immediately after 1 week of Ang-II infusion with a significant increase of the systolic blood pressure (SBP). The SBP in TNFR1-KO mice increased slower within the 2nd and 4th week of Ang-II treatment, but ultimately to similar levels as seen in WT mice (Figure 15). In the WT heart, the body weight-to-heart weight ratio was significant increased after 6 weeks of Ang-II exposure. In TNFR1-KO hearts, the ratio was increased over baseline, but significantly less than in WT hearts (Figure 16.A). The transcriptional expression of hypertrophy-related markers atrial natriuretic peptide (ANP; Figure 16.B) and β-myosin heavy chain (b-MHC, Figure 16.C) was highly upregulated in the WT hearts after 6 weeks of Ang-II infusion. These genes were increased over baseline in Ang-II treated TNFR1-KO hearts, but significantly less than in the WT hearts. These data indicated that both WT and TNFR1-KO mice developed hypertrophy in response to Ang-II; hence these changes were significantly more pronounced in WT mice. To support these results we performed echocardiographic and Doppler Ultrasound studies.

Ang-II was clearly affecting cardiac remodeling in WT mice, while changes in TNFR1-KO animals were minimal. Cardiac hypertrophy and dilation were considerably increased in the WT group (Table 9). The measurement of the left ventricular posterior wall thickness-diastole (LVPW-d) shows that the WT hearts hypertrophied, most likely to compensate the increased afterload caused by Ang-II. The left ventricular end-diastolic diameter (LVEDD) went up significantly in the WT, but not in the TNFR1-KO suggesting volume overload in the WT mice. However, systolic function (LVESD and LVESV) remained the same in both groups. Stroke volume increase was secondary to the increase in the cardiac dimensions and not secondary to pump improvement (Table 9). After 6 weeks of Ang-II, Doppler studies showed that both groups remained essentially without major changes in cardiac function (Table 10). There was no significant difference between WT and TNFR1-KO mice after 6 weeks, diastolic function remained the same. Peak velocity shows a difference between the two groups, but individual increased values are not indicative by itself, as multiple parameters should be considered to obtain proper conclusions.

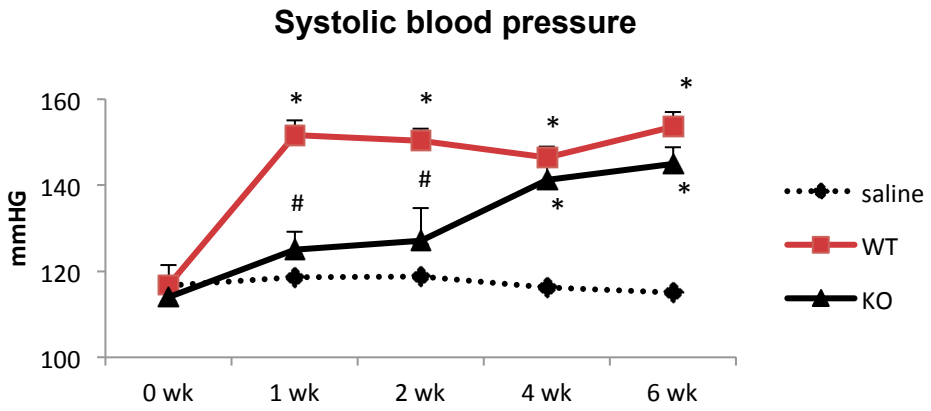

Figure 15: Systolic Blood Pressure
Systolic blood pressure was measured by tail-cuff plethysmography. WT and TNFR1-KO mice developed hypertension in response to Ang-II after 6 weeks. Data for WT (N=3) and TNFR1-KO (N=3) saline groups were pooled for clarity, as there were no differences. WT: N=6; TNFR1-KO: N=8. * P< 0.05 between saline and Ang-II-treated groups within the same genotype group. # P< 0.05 between WT and TNFR1-KO at the same time point.

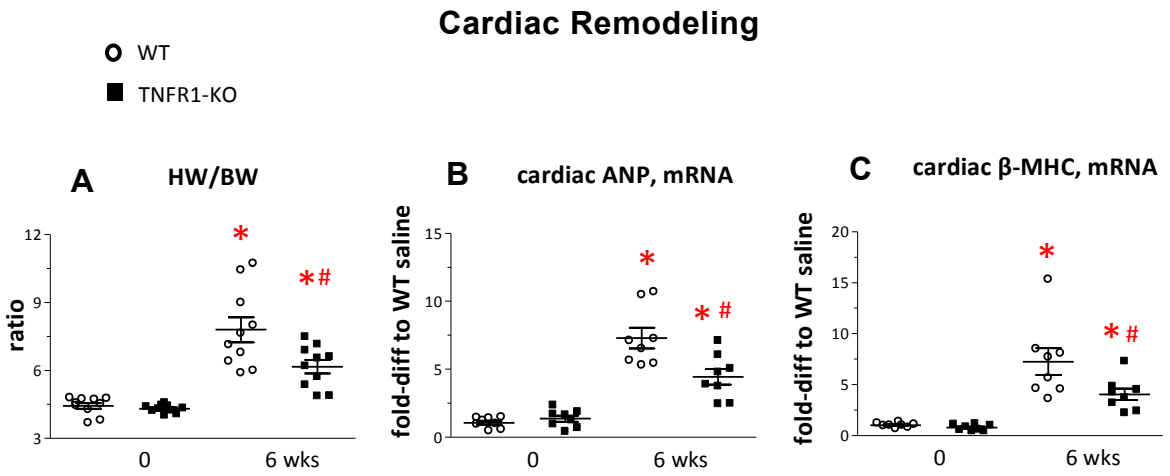

Figure 16: Markers of Hypertrophy
(A) The increase in heart weight-to-body weight ratio, and in transcriptional expression of **(B)** atrial natriuretic peptide (ANP) and **(C)** beta-myosin heavy chain (β-MHC) was higher in WT hearts than in TNFR1-KO hearts. N=8-10/group. * P< 0.05 between saline and 6-week time point within the same genotype group. # P< 0.05 between WT and TNFR1-KO at the same time point.

Echocardiographic and Doppler Ultrasound

	WT	WT	WT	TNFR1-KO	TNFR1-KO	TNFR1-KO
	baseline	6 wks	% change	baseline	6 wks	% change
n	12	12	12	13	13	13
BW, g	25.3 ± 1.6	25.7 ± 1.3	1 ± 5	21.5 ± 1.8 #	22.4 ± 1.7 #	5 ± 6 †
HR, bpm	437 ± 51	532 ± 55 *	25 ± 30	421 ± 38	510 ± 85 *	21 ± 17

Table 8: Global Parameters
* P< 0.05 between saline and6-week Ang-II treatment within the same genotype group
† P< 0.05 between 1 week and 6 weeks within the same genotype group
# P< 0.05 between WT and TNFR1-KO at the same time point
BW= body weight, HR= heart rate

	WT	WT	WT	TNFR1-KO	TNFR1-KO	TNFR1-KO
	baseline	6 wks	% change	baseline	6 wks	% change
n	12	12	12	13	13	13
LVEDD, mm	3.98 ± 0.07	4.35 ± 0.15 *	9 ± 4	3.78 ± 0.08	3.89 ± 0.11 #	3 ± 1
LVEDV, mm^3	69.6 ± 3.0	87.0 ± 6.7 *	26 ± 9	61.7 ± 3.0	66.3 ± 4.3 #	7 ± 4
LVESD, mm	3.04 ± 0.08	3.25 ± 0.15	7 ± 5	2.88 ± 0.09	2.75 ± 0.16 #	5 ± 3 †
LVESV, mm^3	36.9 ± 2.1	40.65 ± 5.0	12 ± 15	30.4 ± 3.0	29.3 ± 3.9	1 ± 13
FS, %	23.3 ± 1.3	29.8 ± 3.1	31 ± 14	26.7 ± 2.1	30.4 ± 2.5	15 ± 6
EF %	46.8 ± 2.3	55.7 ± 4.1	21 ± 10	52.2 ± 3.2	57.4 ± 3.6	11 ± 5
SV, µl	32.7 ± 2.2	46.4 ± 3.16*	45 ± 10	31.4 ± 1.3	37.0 ± 2.2 6 *#	18 ± 5 †
LVPW-d, mm	0.74 ± 0.02	0.88 ± 0.06 *	20 ± 7	0.71 ± 0.04	0.72 ± 0.04 #	3 ± 5 †

Table 9: Echocardiographic Parameters
* P< 0.05 between saline and6-week Ang-II treatment within the same genotype group
† P< 0.05 between 1 week and 6 weeks within the same genotype group
# P< 0.05 between WT and TNFR1-KO at the same time point
LVEDD: left ventricular end diastolic diameter, LVEDV: left ventricular end-diastolic volume, LVESD: left ventricular end-systolic diameters, LVESV: left ventricular end-systolic volume, FS: fractional shortening, EF: ejection fraction, SV: stroke volume, LVPW: left ventricular posterior wall thickness in diastole

	WT	WT	WT	TNFR1-KO	TNFR1-KO	TNFR1-KO
	baseline	6 wks	% change	baseline	6 wks	% change
n	12	12	12	13	13	13
E-Peak Vel, cm/s	79.9 ± 9.2	78.6 ± 16.9	-1 ± 25	75.4 ± 11.2	75.9 ± 16.7	1 ± 15
Peak Vel, cm/s	107 ± 16	146 ± 12 *	39 ± 22	92 ± 14 #	127 ± 36 *	37 ± 32

Table 10: Doppler Parameters
* P< 0.05 between saline and6-week Ang-II treatment within the same genotype group
† P< 0.05 between 1 week and 6 weeks within the same genotype group
# P< 0.05 between WT and TNFR1-KO at the same time point
E-Peak Vel: E- peak velocity, Peak Vel: peak velocity

4.6 In vitro Differentiation of Mouse Monocytes to Fibroblasts in Response to Ang-II and TNF

Freshly isolated mouse monocytes were set atop an endothelial cell layer; MCP-1 was placed beneath in the bottom well. Cells were allowed to migrate through the endothelial cells in response to MCP-1 for 4-6 days (see Figure 4). Some of the successfully migrated cells differentiated into fibroblasts. Fibroblasts were distinguished from other cells by their spindle shaped and elongated morphology; macrophages are round and have a central nucleus. The amount of fibroblasts in unstimulated conditions was designated as “baseline” and the fold increase evoked by Ang-II and TNF stimulation was calculated. As previously shown,[14] Ang-II and TNF stimulation of WT monocytes doubled the number of fibroblasts found in the bottom well. However, Ang-II and TNF stimulation did not induce increased fibroblast formation from TNFR1-KO monocytes. In the current experiment we expanded our observations by using monocytes from TNFR2-deficient mice. As shown in Figure 17, we found that Ang-II and TNF increased the amount of fibroblasts from TNFR2-KO monocytes to similar levels as seen in WT monocytes, indicating that TNFR2 was not involved in the Ang-II/TNF-stimulated fibroblast differentiation.

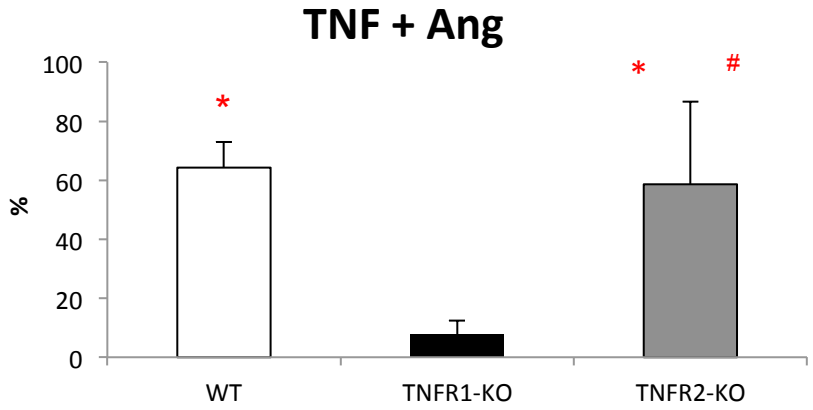

Figure 17: In vitro Monocyte-to-Fibroblast Differentiation Assay:
After successful migration of monocytes through cardiac endothelial cells in response to MCP-1, differentiation into fibroblasts in response to Ang-II and TNF was evaluated. Results are shown as increased percentage over unstimulated numbers (setups that did not received Ang-II and TNF = 0%). N=3-4/group.

5. DISCUSSION

This work focused on a murine model of Ang-II infusion and investigated pro-inflammatory and pro-fibrotic factors involved in differentiation of monocytic precursor cells into fibroblasts in heart and kidney. Previous studies in the heart have shown that MCP-1 was upregulated by short-term Ang-II infusion and induced the uptake of myeloid fibroblast precursor cells into the heart.[9] MCP-1 was required for the uptake of this myeloid cell population, as these cells were absent in hearts of mice deficient in MCP-1 (MCP-1-KO mice).[9] Also, the expression of TNF was obviated in MCP-1-KO hearts after Ang-II exposure. Because other studies reported pro-inflammatory and pro-fibrotic properties for TNF,[18,21] we were interested in whether TNF was involved in the Ang-II-mediated inflammatory response that results in fibrosis.

TNF is known to induce the secretion of chemokines, cytokines, and growth factors on diverse cells including cells of the immune system and specific tissue cells. TNF also affects cell differentiation.[31,32] TNF may signal through two distinct receptors TNFR1 and TNFR2 which mainly differ in their intracellular domains, thus eliciting different physiological responses.[19] TNFR1 has an intracellular death domain region and is mostly regarded as the pro-inflammatory receptor of TNF.[19] TNFR2 is believed to mediate the protective effects of TNF signaling, but its mechanisms have not yet been fully characterized.[18,19]

To explore the role of TNF in Ang-II-mediated cardiac fibrosis, we used mice deficient in either TNFR1 or TNFR2 signaling. We found that TNFR1-KO mice did not develop Ang-II-induced cardiac fibrosis, while TNFR2-KO mice were unaffected and not different than WT mice in any parameter measured.[14] Further, Ang-II infusion to WT mice increased the transcriptional expression of fibrosis- and inflammation- related genes which was absent in TNFR1-KO hearts. Ang-II-infused TNFR1-KO hearts also lacked the presence of collagen-producing, pro-fibrotic M2 cells, yet pro-inflammatory M1 cell uptake was unaffected.[15]

In our current report, we specifically focused on characterizing long-term effects of Ang-II-infusion on cardiac fibrosis. We found that collagen deposition in the heart was maintained over the extended infusion period, however, the inflammatory response dissipated early. Specifically, pro-inflammatory TNF and MCP-1 transcription was absent in WT hearts after 6 weeks of Ang-II exposure. Pro-fibrotic gene expression such as collagen type I and III, α-SMA, osteopontin, and TGF-β1, however, were still activated, albeit at much lower levels than after short-term Ang-II infusion.[14]

In our previous studies using short-term Ang-II infusion, we showed an increase of $CD86^+$ cells in the WT heart 3 days after Ang-II infusion.[15] CD86 and CD16 are a markers for pro-inflammatory M1 cells;[33] we further showed that these cells produce TNF. After 7 days of Ang-II exposure, the amount of M1 cells decreased, whereas a

high number of collagen producing, $CD301^+$, and $CD206^+$ M2 cells were present.[15] In our current study we now demonstrated that after 6 weeks, $CD34^+CD45^+$ fibroblast precursor cells, $CD86^+CD45^+$ and $CD16^+CD45^+$ pro-inflammatory M1 cells, and $CD301^+CD45^+$, $CD206^+CD45^+$, and $CD150^+CD45^+$ pro-fibrotic M2 cells were not present the heart. Together with the fact that MCP-1 was also not upregulated at the 6-week time point, these data support our hypothesis that Ang-II-induced cardiac fibrosis is initiated by an MCP-1-dependent uptake of myeloid fibroblast precursor cells, but that this response resolves over time and progression and maintenance of cardiac fibrosis depends on other mechanisms independent of this cell population. The characterization of such mechanisms is currently focus of our ongoing studies.

Ang-II also induces cardiac remodeling.[34] We previously showed that TNFR1-KO mice were protected from the development of hypertension, cardiac hypertrophy, and LV remodeling and dysfunction after brief infusion of Ang-II.[14] Our current long-term experiments still demonstrate a beneficial effect in the absence of TNFR1 signaling, yet the differences were less pronounced. As discussed above, mice deficient in TNFR1 signaling have still not develop cardiac fibrosis, but showed a tendency of increased hypertrophy and LV remolding after 6 weeks of Ang-II infusion compared to saline-treated TNFR1-KO hearts. However, the extent of these developments was much smaller than in WT at the same time point, and thus numbers were significantly lower. It will have to be tested whether even longer exposure of Ang-II up to several months will overcome the observed protective effects and TNFR1-KO mice will eventually “catch up” with the WT group, or if TNFR1-KO mice will stay protected over time.

Of note, neither mouse group developed significant systolic or diastolic dysfunction due to long-term Ang-II exposure. However, it has to be noted that after short-term Ang-II infusion, we observed worse cardiac performance in WT mice than in TNFR1-KO mice. The reasons for these observations are not known; hence we may assume that lack of TNFR1 may confer a short-term benefit to overcome the sudden increase in Ang-II concentration. Yet in essence, both mouse groups were able to adequately compensate, at least at the 6-week time point. Again, it will have to be tested if Ang-II exposure up to several months will deteriorate cardiac function and if lack of TNFR1 signaling will be of benefit in inhibiting such pathophysiological changes over long time periods.

As for systolic blood pressure, we previously showed that after 1 week of Ang-II infusion, SBP in TNFR1-KO mice remained low, whereas in WT mice SBP increased within a few days to maximal levels. However, in your current study, we found that SBP in the TNFR1-KO mice increased after 2-4 weeks of Ang-II exposure to similar levels as seen in Ang-II-infused WT animals. Therefore, lack of TNFR1 signaling delayed the development of hypertension, but did not prevent it. Importantly however,

the absence of cardiac fibrosis in TNFR1-KO mice after long-term Ang-II infusion despite increased SBP indicated that there may not be a direct correlation between high blood pressure and the development of cardiac fibrosis, as suggested by the current literature.

Since Ang-II is mainly produced and regulated by the kidney, in the current study we were also interested how high levels of Ang-II affects renal fibrosis and function, and specifically if TNFR1 signaling was also a decisive component of these mechanisms. We therefore harvested kidneys from short- and long- term Ang-II-infused mice and characterized mechanisms of renal fibrosis. To understand the importance of our current studies, it is worth noting that most, if not all, Ang-II infusion studies described in the literature used a secondary injury, such as uninephrectomy or high-salt diet, to enhance the negative effects of Ang-II on the kidney.[35] Therefore, our study is the first, to our knowledge, that investigated effects solemnly due to Ang-II exposure.

We found the kidney to be quite robust against Ang-II-exposure; perhaps for this reason other laboratories used additional methods to augment its effects. First of all, we found no fibrosis in the kidney after short-term Ang-II infusion. Renal fibrosis slowly developed by 6 weeks of infusion, however, the extent of fibrosis (as measured by collagen deposition and pro-fibrotic gene activation), although significant, was lower than observed in the heart at the same time point. Still, we found an increase in MCP-1 and TNF expression in the kidney, as well as the concurrent presence of monocytic fibroblast precursors, pro-inflammatory M1, and pro-fibrotic M2 cells in the kidney, the latter also producing collagen type I. These data indicated that renal fibrosis may be initiated by similar mechanisms as in the heart, involving the MCP-1-dependent uptake of myeloid fibroblast precursor cells that differentiated into collagen-producing fibroblasts, yet due to the kidney's robustness, the activation of these mechanisms was much slower than those in the heart. Further studies are necessary to confirm our hypothesis, as well as to expand our observations to elucidate more mechanistic details leading to kidney fibrosis.

BUN and creatinine are two well-known serum markers of kidney failure.[27] In our model, neither marker was augmented after short-term Ang-II infusion, but both increased after 6 weeks. Furthermore their levels did not differ between WT and TNFR1-KO mice, indicating that both mouse groups showed a decline in renal function to similar extents. However, histologic examination of Ang-II-infused kidney samples did not reveal noticeable irregularities in the tissue structure in neither mouse group compared to saline-treated groups. The reasons for this observation are unknown; most probably, at this time point, the negative effects of renal fibrosis and failure are still too weak to elicit visible changes in kidney structure and longer times of Ang-II infusion may be necessary to observe significant structural changes.

Over the last years, in parallel to our various in vivo studies, we also developed an in vitro model of monocyte-to-fibroblast differentiation to supplement our in vivo observations. This model enables us to dissect specific mechanisms of myeloid fibroblast formation. As published in numerous studies, we found that this assay reliably predicts and verifies effectors of myeloid fibroblasts formation involved in adverse cardiac remodeling, as this assay allows a more careful examination of the quantitative, qualitative, and temporal aspects of myeloid fibroblast formation that cannot be directly addressed in vivo. Using this assay, we were able to establish the requirement of TNF for the development of Ang-II-induced fibrosis in a controlled environment. Specifically, we showed that both Ang-II and TNF had to be present together, as each factor alone did not increase fibroblast formation.[14]

In those studies, we have used human monocytes in order to establish a relationship with human disease.[22,23] We were therefore bound to commercially available human antibodies to specially engage or block our receptor of interest in order to investigate its involvement in fibroblast maturation. In our most recent,[15] as well as in our current study, we presented a new and updated method of isolating mouse monocytes from spleen and optimization of our TEM conditions, including the use of mouse endothelial cells. Thus, we were previously able to demonstrate the involvement of TNFR1 in Ang-II-induced monocyte-to-fibroblast maturation by using cells from TNFR1-KO mice, as these cells did not mature into firboblats.[14] In the current study we expanded these observations by using monocytes isolated from TNFR2-KO spleen and showing that the amount of fibroblasts generated with these cells was not different than the amount generated by WT monocytes, but was significantly higher than those from TNFR1-KO mice. These data are important as the last convincing piece indicating that TNFR2 signaling is not involved in the Ang-II-mediated fibrosis, and complement our previously published in vivo experiments.[14]

6. CONCLUSION

The fibrotic response in the heart occurred immediately after Ang-II exposure while fibrosis in the kidney developed slowly. Yet both were initiated by the MCP-1-mediated uptake of bone marrow-derived fibroblast precursors. TNFR1-KO mice were protected from the Ang-II induced cardiac and renal fibrosis.

In the heart, upregulation of MCP-1 and presence of fibroblast precursor cells dissipated quickly, however, the fibrosis persisted. These data indicated that the monocytic fibroblast precursor population was necessary for the initiation of the fibrotic development, but other mechanisms were responsible for its maintenance and progression. TNFR1-KO mice were protected from cardiac fibrosis even after Ang-II infusion of 6 weeks, despite development of hypertension similar to WT levels. In addition, the Ang-II-induced development of hypertrophy was significantly more pronounced in WT hearts than in TNFR1-KO hearts.

The kidney seems to be a much more robust organ than the heart, as renal fibrosis and failure developed slowly in responds to Ang-II exposure, yet lack of TNFR1 signaling seemed to be protective as well. Experiments involving longer exposure periods of Ang-II may be necessary for elucidating more detailed mechanistic aspects.

In summary the lack of TNFR1 signaling protects against Ang-II-induced cardiac and renal fibrosis, and cardiac hypertrophy and remodeling, but cannot prevent systemic alterations such development of hypertension and renal dysfunction.

7. REFERENCES

1. American Heart Association, American Stroke Association. Heart Disease and Stroke Statistics. 2005;(1):53.

2. Nichols M, Townsend N, Scarborough P, Rayner M. Cardiovascular disease in Europe: Epidemiological update. *Eur Heart J*. 2013;34(39):3028-3034. doi:10.1093/eurheartj/eht356.

3. Katz DH, Beussink L, Sauer AJ, Freed BH, Burke MA, Shah SJ. Prevalence, clinical characteristics, and outcomes associated with eccentric versus concentric left ventricular hypertrophy in heart failure with preserved ejection fraction. *Am J Cardiol*. 2013;112(8):1158-1164. doi:10.1016/j.amjcard.2013.05.061.

4. TAKANO H, HASEGAWA H, NAGAI T, KOMURO I. Implication of Cardiac Remodeling in Heart Failure: Mechanisms and Therapeutic Strategies. *Intern Med*. 2003;42(6):465-469. doi:10.2169/internalmedicine.42.465.

5. Porter KE, Turner NA. Cardiac fibroblasts: at the heart of myocardial remodeling. *Pharmacol Ther*. 2009;123(2):255-278. doi:10.1016/j.pharmthera.2009.05.002.

6. Weber KT, Brilla CG. Pathological hypertrophy and cardiac interstitium. Fibrosis and renin-angiotensin-aldosterone system. *Circulation*. 1991;83(6):1849-1865. http://www.ncbi.nlm.nih.gov/pubmed/1828192. Accessed July 31, 2015.

7. Kuwahara F, Kai H, Tokuda K, et al. Hypertensive myocardial fibrosis and diastolic dysfunction: another model of inflammation? *Hypertension*. 2004;43(4):739-745. doi:10.1161/01.HYP.0000118584.33350.7d.

8. Haudek SB, Xia Y, Huebener P, et al. Bone marrow-derived fibroblast precursors mediate ischemic cardiomyopathy in mice. *Proc Natl Acad Sci U S A*. 2006;103(48):18284-18289. doi:10.1073/pnas.0608799103.

9. Haudek SB, Cheng J, Du J, et al. Monocytic fibroblast precursors mediate fibrosis in angiotensin-II-induced cardiac hypertrophy. *J Mol Cell Cardiol*. 2010;49(3):499-507. doi:10.1016/j.yjmcc.2010.05.005.

10. Angiotensin II Type 1 Receptor Gene Polymorphisms in Human Essential Hypertension. http://hyper.ahajournals.org/content/24/1/63.full.pdf. Accessed August 19, 2015.

11. Mann DL. Angiotensin II as an Inflammatory Mediator: Evolving Concepts in the Role of the Renin Angiotensin System in the Failing Heart. *Cardiovasc Drugs Ther*. 16(1):7-9. doi:10.1023/A:1015355112501.

12. *Fibrogenesis: Cellular and Molecular Basis*. Springer Science & Business Media; 2007. https://books.google.com/books?id=RwGarwpTRXgC&pgis=1. Accessed September 21, 2015.

13. Branton MH, Kopp JB. TGF-beta and fibrosis. *Microbes Infect*. 1999;1(15):1349-1365. http://www.ncbi.nlm.nih.gov/pubmed/10611762. Accessed September 21, 2015.

14. Duerrschmid C, Crawford JR, Reineke E, et al. TNF receptor 1 signaling is critically involved in mediating angiotensin-II-induced cardiac fibrosis. *J Mol Cell Cardiol*. 2013;57:59-67. doi:10.1016/j.yjmcc.2013.01.006.

15. Duerrschmid C, Trial J, Wang Y, Entman ML, Haudek SB. Tumor necrosis factor: a mechanistic link between angiotensin-II-Induced cardiac inflammation and fibrosis. *Circ Heart Fail*. 2015;8(2):352-361. doi:10.1161/CIRCHEARTFAILURE.114.001893.

16. Hehlgans T, Pfeffer K. The intriguing biology of the tumour necrosis factor/tumour necrosis factor receptor superfamily: players, rules and the games. *Immunology*. 2005;115(1):1-20. doi:10.1111/j.1365-2567.2005.02143.x.

17. Clark J, Vagenas P, Panesar M, Cope AP. What does tumour necrosis factor excess do to the immune system long term? *Ann Rheum Dis*. 2005;64 Suppl 4:iv70-iv76. doi:10.1136/ard.2005.042523.

18. Kleinbongard P, Heusch G, Schulz R. TNFalpha in atherosclerosis, myocardial ischemia/reperfusion and heart failure. *Pharmacol Ther*. 2010;127(3):295-314. doi:10.1016/j.pharmthera.2010.05.002.

19. Cabal-Hierro L, Lazo PS. Signal transduction by tumor necrosis factor receptors. *Cell Signal*. 2012;24(6):1297-1305. doi:10.1016/j.cellsig.2012.02.006.

20. Schulz R, Heusch G. Tumor necrosis factor-alpha and its receptors 1 and 2: Yin and Yang in myocardial infarction? *Circulation*. 2009;119(10):1355-1357. doi:10.1161/CIRCULATIONAHA.108.846105.

21. Distler JHW, Schett G, Gay S, Distler O. The controversial role of tumor necrosis factor alpha in fibrotic diseases. *Arthritis Rheum*. 2008;58(8):2228-2235. doi:10.1002/art.23645.

22. Haudek SB, Trial J, Xia Y, Gupta D, Pilling D, Entman ML. Fc receptor engagement mediates differentiation of cardiac fibroblast precursor cells. PNAS 2008;105:10179-10184.

23. Trial J, Cieslik KA, Haudek SB, Duerrschmid C, Entman ML. Th1/M1 conversion to th2/m2 responses in models of inflammation lacking cell death stimulates maturation of monocyte precursors to fibroblasts. Front Immunol 2013;4:287.

24. ALZET® Osmotic Pumps - Implantable pumps for research. http://www.alzet.com/. Accessed July 28, 2015.

25. Bustin SA, Benes V, Garson JA, et al. The MIQE guidelines: minimum information for publication of quantitative real-time PCR experiments. *Clin Chem*. 2009;55(4):611-622. doi:10.1373/clinchem.2008.112797.

26 Hosten AO. BUN and Creatinine. 1990. http://www.ncbi.nlm.nih.gov/books/NBK305/. Accessed July 2, 2015.

27. Biochemistry and Medical Genetics. https://fgq77.files.wordpress.com/2010/10/kaplan-biochemistry-2006.pdf. Accessed July 29, 2015.

28. Cardiac Endothelial. http://www.cellutionsbiosystems.com/index.php?option=com_virtuemart&page=shop.browse&category_id=10&Itemid=40. Accessed July 28, 2015.

29. EasySep™ Mouse Monocyte Enrichment Kit. http://www.stemcell.com/en/Products/All-Products/EasySep-Mouse-Monocyte-Enrichment-Kit.aspx. Accessed July 6, 2015.

30. Visitech Systems. http://www.visitechsystems.com/. Accessed July 28, 2015.

31. Chesney J, Metz C, Stavitsky AB, Bacher M, Bucala R. Regulated production of type I collagen and inflammatory cytokines by peripheral blood fibrocytes. *J Immunol*. 1998;160(1):419-425. http://www.ncbi.nlm.nih.gov/pubmed/9551999. Accessed September 24, 2015.

32. Chomarat P, Dantin C, Bennett L, Banchereau J, Palucka AK. TNF skews monocyte differentiation from macrophages to dendritic cells. *J Immunol*. 2003;171(5):2262-2269. http://www.ncbi.nlm.nih.gov/pubmed/12928370. Accessed September 24, 2015.

33. Mosser DM. The many faces of macrophage activation. *J Leukoc Biol*. 2003;73(2):209-212. http://www.ncbi.nlm.nih.gov/pubmed/12554797. Accessed June 29, 2015.

34. Jia L, Li Y, Xiao C, Du J. Angiotensin II induces inflammation leading to cardiac remodeling. *Front Biosci (Landmark Ed*. 2012;17:221-231. http://www.ncbi.nlm.nih.gov/pubmed/22201740. Accessed September 30, 2015.

35. Xia Y, Entman ML, Wang Y. Critical role of CXCL16 in hypertensive kidney injury and fibrosis. *Hypertension*. 2013;62(6):1129-1137. doi:10.1161/HYPERTENSIONAHA.113.01837.

8. FIGURES

9. TABLES